Short- and long-read metagenomics of South African gut microbiomes reveal a transitional composition and novel taxa

Fiona B. Tamburini[1], Dylan Maghini[1], Ovokeraye H. Oduaran[2], Ryan Brewster[3], Michaella R. Hulley[2,4], Venesa Sahibdeen[4], Shane A. Norris[5,6], Stephen Tollman[7,8], Kathleen Kahn[7,8], Ryan G. Wagner[7,8], Alisha N. Wade[7], Floidy Wafawanaka[7], Xavier Gómez-Olivé[7,8], Rhian Twine[7], Zané Lombard[4], Scott Hazelhurst[2,9*], Ami S. Bhatt[1,3,10*]┼

[1]Department of Genetics, Stanford University, Stanford, CA, USA

[2]Sydney Brenner Institute for Molecular Bioscience, University of the Witwatersrand, Johannesburg, South Africa

[3]School of Medicine, Stanford University, Stanford, CA, USA

[4]Division of Human Genetics, School of Pathology, Faculty of Health Sciences, National Health Laboratory Service & University of the Witwatersrand, Johannesburg, South Africa

[5]SAMRC Developmental Pathways for Health Research Unit, Department of Paediatrics, University of the Witwatersrand, Johannesburg, South Africa

[6]School of Human Development and Health, University of Southampton, UK

[7]MRC/Wits Rural Public Health and Health Transitions Research Unit (Agincourt), School of Public Health, Faculty of Health Sciences, University of the Witwatersrand, Johannesburg, South Africa

[8]INDEPTH Network, East Legon, Accra, Ghana

[9]School of Electrical and Information Engineering, University of the Witwatersrand, Johannesburg, South Africa

[10]Department of Medicine (Hematology, Blood and Marrow Transplantation), Stanford University, Stanford, CA, USA

*Co-corresponding authors: asbhatt@stanford.edu, Scott.Hazelhurst@wits.ac.za

┼Lead contact

Abstract

While human gut microbiome research often focuses on western populations or nonwestern agriculturalist and hunter-gatherer societies, most of the world's population resides between these extremes. We present the first study evaluating gut microbiome composition in transitioning South African populations using short- and long-read sequencing. We analyzed stool samples from adult females (age 40 - 72) living in rural Bushbuckridge municipality (n=117) or urban Soweto (n=51) and find that these microbiomes are intermediate between those of western industrialized and previously studied non-industrialized African populations. We demonstrate that reference collections are incomplete for nonwestern microbiomes, resulting in within-cohort beta diversity patterns that are in some cases reversed compared to reference-agnostic sequence comparison patterns. To improve reference databases, we generated complete genomes of undescribed taxa, including *Treponema*, *Lentisphaerae*, and *Succinatimonas* species. Our results suggest that South Africa's transitional lifestyle and epidemiological conditions are reflected in gut microbiota compositions, and that these populations contain microbial diversity that remains to be described.

Introduction

Comprehensive characterization of the full diversity of the healthy human gut microbiota is essential to contextualize studies of the microbiome in disease. To date, substantial resources have been invested in describing the microbiome of individuals living in the global 'west' (United States, northern and western Europe), including efforts by large consortia such as the Human Microbiome Project (Human Microbiome Project Consortium, 2012) and metaHIT (Qin et al., 2010). Though these projects have yielded valuable descriptions of human gut microbial ecology, they survey only a small portion of the world's citizens at the extreme of industrialized, urbanized lifestyle. It is unclear to what extent these results are generalizable to non-western and non-industrialized populations across the globe.

At the other extreme, a relatively smaller number of studies have characterized the gut microbiome composition of non-western individuals practicing traditional lifestyles (Brewster et al., 2019; Gupta et al., 2017), including communities in Venezuela and Malawi (Yatsunenko et al., 2012), hunter-gatherer communities in Tanzania (Fragiadakis et al., 2018; Rampelli et al., 2015; Schnorr et al., 2014; Smits et al., 2017), non-industrialized populations in Tanzania and Botswana (Hansen et al., 2019), and agriculturalists in Peru (Obregon-Tito et al., 2015) and remote Madagascar (Pasolli et al., 2019). However, these cohorts are not representative of how most of the world lives either. Many of the world's communities lead lifestyles between the extremes of an urbanized, industrialized lifestyle and traditional practices. It is a scientific and ethical imperative to include these diverse populations in biomedical research, yet dismayingly many of these intermediate groups are underrepresented or absent from the published microbiome literature.

This major gap in our knowledge of the human gut microbiome leaves the biomedical research community ill-poised to relate microbiome composition to human health and disease across the breadth of the world's population. Worldwide, many communities are currently undergoing a transition of diet and lifestyle practice, characterized by increased access to processed foods, diets rich in animal fats and simple carbohydrates, and more sedentary lifestyles (Vangay et al., 2018). This has corresponded with an epidemiological transition in which the burden of disease is shifting from predominantly infectious diseases to include increasing incidence of noncommunicable diseases like obesity and diabetes (Collinson et al., 2014). The microbiome has been implicated in various noncommunicable diseases (Griffiths and Mazmanian, 2018; Helmink et al., 2019; Turnbaugh et al., 2009) and may mediate the efficacy of medical interventions including vaccines (Ciabattini et al., 2019; Hagan et al., 2019), but we cannot evaluate the generalizability of these findings without establishing baseline microbiome characteristics of communities that practice diverse lifestyles and by extension, harbor diverse microbiota. These understudied populations offer a unique opportunity to examine the relationship between lifestyle (including diet), disease, and gut microbiome composition, and to discover novel microbial genomic content.

A few previous studies have begun to probe the relationship between lifestyle and microbiome composition in transitional communities (de la Cuesta-Zuluaga et al., 2018; Gupta et al., 2017; Jha et al., 2018; Ou et al., 2013). However, substantial gaps remain in our description of the microbiome in transitional communities. In particular, knowledge of the gut microbiota on the African continent is remarkably sparse. In fact, of 60 studies surveying the gut microbiome in African populations as of mid-2020 (Table S1), 34 (57%) have focused entirely on on children or infants, whose disease risk profile and gut microbiome composition can vary considerably from adults (Lim et al., 2012; Yatsunenko et al., 2012). Additionally, 52 of 60 (87%) of studies of the gut microbiome in Africans employed 16S rRNA gene sequencing or qPCR, techniques which amplify only a tiny portion of the genome and therefore lack genomic resolution to describe species or strains which may share a 16S rRNA sequence but differ in gene content or genome structure. To our knowledge, only five published studies to date have used shotgun metagenomics to describe the gut microbiome of adult populations living in Africa (Campbell et al., 2020; Lokmer et al., 2019; Pasolli et al., 2019; Rampelli et al., 2015; Smits et al., 2017).

To address this major knowledge gap, we designed and performed the first research study applying short- and long-read DNA sequencing to study the gut microbiomes of South African individuals for whom 16S rRNA gene sequence data has recently been reported (Oduaran et al., 2020). South Africa is a prime example of a country undergoing rapid lifestyle and epidemiological transition. With the exception of the HIV/AIDS epidemic in the mid-1990s to the mid-2000s, over the past three decades South Africa has experienced a steadily decreasing mortality from infectious disease and an increase in noncommunicable disease (Kabudula et al., 2017a; Santosa and Byass, 2016). Concomitantly, increasingly sedentary lifestyles and changes in dietary habits, including access to calorie-dense processed foods, contribute to a higher prevalence of obesity in many regions of South Africa (Kabudula et al., 2017a), a trend which disproportionately affects women (Ajayi et al., 2016; NCD Risk Factor Collaboration (NCD-RisC) – Africa Working Group, 2017).

This study represents the largest shotgun metagenomic dataset of African adults in the published literature to date. In this work, we describe microbial community-scale similarities between urban and rural communities in South Africa, as well as distinct hallmark taxa that distinguish each community. Additionally, we place South Africans in context with microbiome data from other populations globally, revealing the transitional nature of gut microbiome composition in the South African cohorts. We demonstrate that metagenomic assembly of short reads yields novel strain and species draft genomes. Finally, we apply Oxford Nanopore long-read sequencing to samples from the rural cohort and generate complete and near-complete genomes. These include genomes of species that are exclusive to, or more prevalent in, traditional populations, including *Treponema* and *Prevotella* species. As long-read sequencing enables more uniform coverage of AT-rich regions compared to short-read sequencing with transposase-based library preparation, we also generate complete metagenome-assembled AT-rich genomes from less well-described gut microbes including species in the phylum *Melainabacteria*, the class *Mollicutes*, and the genus *Mycoplasma*.

Taken together, the results herein offer a more detailed description of gut microbiome composition in understudied transitioning populations, and present complete and contiguous reference genomes that will enable further studies of gut microbiota in nonwestern populations. Importantly, this study was developed with an ethical commitment to engaging both rural and urban community members to ensure that the research was conducted equitably (more details in Supplemental Information). This work underscores the critical need to broaden the scope of human gut microbiome research and include understudied, nonwestern populations to improve the relevance and accuracy of microbiome discoveries to broader populations.

Results

Cohorts and sample collection

We enrolled 190 women aged between 40-72, living in rural villages in the Bushbuckridge Municipality (31.26°E, 24.82°S, n=132) and urban Soweto, Johannesburg (26.25°S, 27.85°E, n=58) and collected a one-time stool sample, as well as point of care blood glucose and blood pressure measurements and a rapid HIV test. Only samples from HIV-negative individuals were analyzed further (n=117 Bushbuckridge, n=51 Soweto). Participants spanned a range of BMI from healthy to overweight; the most common comorbidity reported was hypertension, and many patients reported taking anti-hypertensive medication (18 of 117 (15%) in Bushbuckridge, 15 of 51 (29%) in Soweto) (Table 1, Table S2). Additional medications are summarized in Table S2. We extracted DNA from each stool sample and conducted 150 base pair (bp) paired-end sequencing on the Illumina HiSeq 4000 platform. A median of 34.5 million (M) raw reads were generated per sample (range 11.4 M - 100 M), and a median of 11.2 M reads (range 3.2 M - 29.3 M) resulted after pre-processing including de-duplication, trimming, and human read removal (Table S3).

Gut microbial composition

We taxonomically classified sequencing reads against a comprehensive custom reference database containing all microbial genomes in RefSeq and GenBank at scaffold quality or better as of January 2020 (177,626 genomes total). Concordant with observations from 16S rRNA gene sequencing of the same samples (Oduaran et al., 2020), we find that *Prevotella*, *Faecalibacterium*, and *Bacteroides* are the most abundant genera in most individuals across both study sites (Figure 1A, Figure S1, Table S4; species-level classifications in Table S5). Additionally, in many individuals we observe taxa that are uncommon in western microbiomes, including members of the VANISH (Volatile and/or Associated Negatively with Industrialized Societies of Humans) taxa (families *Prevotellaceae*, *Succinovibrionaceae*, *Paraprevotellaceae*, and *Spirochaetaceae*) (Fragiadakis et al., 2018) such as *Prevotella, Treponema*, and *Succinatimonas*, which have been demonstrated to be higher in relative abundance in communities practicing traditional lifestyles compared to westerners (Fragiadakis et al., 2018; Sonnenburg and Sonnenburg, 2019) (Figure 1B, Table S4). The mean relative abundance of each VANISH genus is higher in Bushbuckridge than Soweto, though the difference is not statistically significant for *Prevotella*, *Paraprevotella*, or *Alkalispirochaeta* (Figure 1B, Wilcoxon rank-sum test). Within the Bushbuckridge cohort, we observe a bimodal distribution of the genera *Succinatimonas*, *Succinivibrio*, and *Treponema* (Figure S2A). While we do not identify any participant metadata that associate with this distribution, we observe that VANISH taxa are weakly correlated with one another in metagenomes from both Bushbuckridge and Soweto (Figure S2B-C).

Intriguingly, we observed that an increased proportion of reads aligned to the human genome during pre-processing in samples from Soweto compared to Bushbuckridge (Figure S3, Wilcoxon rank sum test $p < 0.0001$). This could potentially indicate higher inflammation and immune cell content or sloughing of intestinal epithelial cells in the urban Soweto cohort compared to rural Bushbuckridge.

Rural and urban microbiomes cluster distinctly in MDS

We hypothesized that lifestyle differences of those residing in rural Bushbuckridge versus urban Soweto might be associated with demonstrable differences in gut microbiome composition. Bushbuckridge and Soweto differ markedly in their population density (53 and 6,357 persons per km^2 respectively as of the 2011 census) as well as in lifestyle variables including the prevalence of flush toilets (6.8 vs 91.6% of dwellings) and piped water (11.9 vs 55% of dwellings) (additional site demographic information in Table S6) (Statistics South Africa, 2012). Soweto is highly urbanized and has been so for several generations, while Bushbuckridge is classified as a rural community, although it is undergoing rapid epidemiological transition. Bushbuckridge also sees circular rural/urban migrancy typified by some (mostly male) members of a rural community working and living for extended periods in urban areas, while keeping their permanent rural home (Ginsburg et al., 2016). Although our participants all live in Bushbuckridge, this migrancy in the community helps make the boundary between rural and urban lifestyles more fluid. Comparing the two study populations at the community level, we find that samples from the two sites have distinct centroids (PERMANOVA $p < 0.001$, $R^2 = 0.037$) but overlap (Figure 2A), though we note that the dispersion of the Soweto samples is greater than that of the Bushbuckridge samples (PERMDISP2 $p < 0.001$). Across the study population we observe a gradient of Bacteroides and Prevotella relative abundance (Figure S4). This is likely a result of differences in diet across the study population at both sites, as Bacteroides and Prevotella have been proposed as biomarkers of diet and lifestyle (De Filippo et al., 2010; Gorvitovskaia et al., 2016; Yatsunenko et al., 2012).

To determine if medication usage was associated with gut microbiome composition, we included each participant's self-reported concomitant medications (summarized in Table S2) to re-visualize the microbiome composition of samples in MDS by class of medication (Figure S5A,B). We find that self-reported medication is not significantly correlated with community composition in this cohort (PERMANOVA $p > 0.05$, Figure S5C) except for in the case of proton pump inhibitors (PPIs) (PERMANOVA $p = 0.026$, $R^2 = 0.0136$). We note that PPIs are one of several drug classes previously found to associate with changes in gut microbiome composition (Maier and Typas, 2017); as only two participants self-report taking PPIs at the time of sampling, additional data is required to evaluate the robustness of this finding in these South African populations.

Rural and urban microbiomes differ in Shannon diversity and species composition

Gut microbiome alpha diversity of individuals living traditional lifestyles has been reported to be higher than those living western lifestyles (De Filippo et al., 2010; Obregon-Tito et al., 2015; Schnorr et al., 2014). In keeping with this general trend, we find that alpha diversity (Shannon) is significantly higher in individuals living in rural Bushbuckridge than urban Soweto (Figure 2B; Wilcoxon rank-sum test, $p < 0.01$). Using DESeq2 to identify microbial genera that are differentially abundant across study sites, we find that genera including *Bacteroides*, *Bifidobacterium,* and *Staphylococcus* are more abundant in individuals living in Soweto (Figure 2C, Table S7, species shown in Figure S6). Interestingly, we find microbial genera enriched in gut microbiomes of individuals living in Bushbuckridge that are common to both the environment and the gut, including *Streptomyces* and *Pseudomonas* (Table S7). Typically a soil-associated organism, *Streptomyces* encode a variety of biosynthetic gene clusters and can produce numerous immunomodulatory and anti-inflammatory compounds such as rapamycin and tacrolimus, and it has been suggested that decreased exposure to *Streptomyces* is associated with increased incidence of inflammatory disease and colon cancer in western populations (Bolourian and Mojtahedi, 2018). In addition, we find enrichment of genera in Bushbuckridge that have been previously associated with nonwestern microbiomes including *Succinatimonas*, a relatively poorly-described bacterial genus with only one type species, and Elusimicrobia, a phylum which has been detected in the gut microbiome of rural Malagasy (Pasolli et al., 2019).

Additionally, Bushbuckridge samples are enriched for Cyanobacteria as well as Candidatus Melainabacter, a phylum closely related to Cyanobacteria that in limited studies has been described to inhabit the human gut (Di Rienzi et al., 2013; Soo et al., 2014)

We find that Bushbuckridge samples have an increased number of bacteriophages (506.1 ± 71.7) compared to samples from Soweto (201.5 ± 39.4; p = 8.606e-10). Interestingly, we identify the bacteriophage crAssphage and related crAss-like phages (Guerin et al., 2018), which have recently been described as prevalent constituents of the gut microbiome globally (Edwards et al., 2019), in 32 of 51 participants (63%) in Soweto and 84 of 117 (72%) in Bushbuckridge (difference in prevalence between cohorts not significant, p = 0.28 Fisher's exact test) using 650 sequence reads or roughly 1X coverage of the 97 kb genome as a threshold for binary categorization of crAss-like phage presence or absence. Prototypical crAssphage has been hypothesized to infect *Bacteroides* species and a crAss-like phage has been demonstrated to infect *Bacteroides intestinalis*. Though crAss-like phages do not differ between cohorts in terms of prevalence (presence/absence), we observe that both crAss-like phages and *Bacteroides* are enriched in relative abundance in the gut microbiome of individuals living in Soweto compared to Bushbuckridge (Figure 2C).

No strong signals of interaction between human DNA variation and microbiome content detected

We have a very small sample size to assess interaction between human genetic variation and microbiome population. However, as our study is one of the relatively few with both human and microbiome DNA characterized, we performed association tests between key microbiome genera abundance levels and the human DNA. After correcting for multiple testing there were only a few SNPs with borderline statistically significant association with genera abundance levels (Table S8). They occur in genomic regions with no obvious impact on the gut microbiome (see Methods/Supplementary Information). Additionally, we do not observe that samples cluster by self-reported ethnicity of the participant (Figure S7).

South African gut microbiomes share taxa with western and nonwestern populations yet harbor distinct features

To place the microbiome composition of South African individuals in global context with metagenomes from healthy adults living in other parts of the world, we compared publicly available data from four cohorts (Figure 3A, Table S9) comprising adult individuals living in the United States (Human Microbiome Project Consortium, 2012), northern Europe (Sweden) (Bäckhed et al., 2015), rural Madagascar (Pasolli et al., 2019), as well as the Hadza hunter-gatherers of Tanzania (Rampelli et al., 2015). We note the caveat that these samples were collected at different times using different approaches, and that there is variation in DNA extraction, sequencing library preparation and sequencing, all of which may contribute to variation between studies. Recognizing this limitation, we observe that South African samples cluster between western and nonwestern populations[1] in MDS (Figure 3B) as expected, and that the first axis of MDS correlates well with geography and lifestyle (Figure 3C). Additionally, the relative abundance of *Streptomycetaceae*, *Spirochaetaceae*, *Succinivibrionaceae*, and *Bacteroidaceae* are most strongly correlated with the first axis of MDS (Spearman's rho > 0.8): *Bacteroidaceae* decreases with MDS 1 while *Streptomycetaceae*, *Spirochaetaceae*, *Succinivibrionaceae* increase (Figure 3B). These observations suggest that the transitional lifestyle of South African individuals is reflected in their gut microbiome composition. We observe a corresponding pattern of decreasing relative abundance of VANISH taxa across lifestyle and geography (Figure S8).

The two South African cohorts also have distinct differences from both nonwestern and western populations, as evidenced by displacement along the second axis of MDS (Figure 3B). To identify the taxa that drive this separation, we analyzed datasets grouped by lifestyle into the general categories of "nonwestern" (Tanzania, Madagascar), "western" (USA, Sweden), and South African (Bushbuckridge and Soweto). We performed statistical analysis using DESeq2 to identify microbial genera that differed significantly in the South African cohort compared to both nonwestern and western categories (with the same directionality of effect in each comparison, e.g. enriched in South Africans compared to both western and nonwestern groups) (Figure S9). We observe that taxa including *Escherichia*, *Lactobacillus*, and *Lactococcus* are lower in relative abundance in South Africans compared to both western and nonwestern categories. Conversely, unclassified bacteria of the phylum Verrucomicrobia are enriched in South Africans. Intriguingly, in this analysis we observe that two crAssphage clades, alpha and delta (Guerin et al., 2018), are lower in abundance in South African participants relative to all other cohorts. This

[1] We use the term "western" to denote western/industrialized populations and "nonwestern" to describe populations not living in the geographic west, as in this case "non-industrialized" does not accurately describe urban Soweto.

may suggest a non-uniform geographic distribution of crAssphage clades and/or crAssphage hosts.

Decreased sequence classifiability in nonwestern populations

Given previous observations that gut microbiome alpha diversity is higher in individuals practicing traditional lifestyles (Gupta et al., 2017; Smits et al., 2017; Sonnenburg and Sonnenburg, 2018) and that immigration from a nonwestern nation to the United States is associated with a decrease in gut microbial alpha diversity (Vangay et al., 2018), we hypothesized that alpha diversity would be higher in nonwestern populations including South Africans. We observe that Shannon diversity of the Tanzanian hunter-gatherer cohort is uniformly higher than all other populations (Figure 3D; $p < 0.01$ for all pairwise comparisons; FDR-adjusted Wilcoxon rank sum test) and that alpha diversity is lower in individuals living in the United States compared to all other cohorts (Figure 3D; $p < 0.0001$ for all pairwise comparisons; FDR-adjusted Wilcoxon rank sum test). Surprisingly, we observe comparable Shannon diversity between Madagascar, Bushbuckridge, and Sweden (ns, Wilcoxon rank sum test). However, this could be an artifact of incomplete representation of diverse microbes in existing reference collections.

Classification of metagenomic sequences from nonwestern gut microbiomes with existing reference collections is known to be limited (Nayfach et al., 2019; Pasolli et al., 2019), and we observe decreased sequence classifiability in nonwestern populations (Figure 4A). Therefore, we sought orthogonal validation of our observation that South African microbiomes represent a transitional state between traditional and western microbiomes and employed a reference-independent method to evaluate the nucleotide composition of sequence data from each metagenome. We used the sourmash workflow (Brown and Irber, 2016) to compare nucleotide *k*-mer composition of sequencing reads in each sample and ordinated based on angular distance, which accounts for *k*-mer abundance. Using a *k*-mer length of 31 (*k*-mer similarity at *k*=31 correlates with species-level similarity (Koslicki and Falush, 2016)), we observe clustering reminiscent of the species ordination plot shown in Fig. 3, further supporting the hypothesis that South African microbiomes are transitional (Figure 4B).

Previous studies have reported a pattern of higher alpha diversity but lower beta diversity in nonwestern populations compared to western populations (Martínez et al., 2015; Schnorr et al., 2014). Hypothesizing that alpha and beta diversity may be underestimated for populations whose gut microbes are not well-represented in reference collections, we compared beta diversity (distributions of within-cohort pairwise distances) calculated via species Bray-Curtis dissimilarity as well as nucleotide *k*-mer angular distance (Figure 4C-E). Of note, beta diversity is highest in Soweto irrespective of distance measure (Figure 4C). Intriguingly, in some cases we observe that the relationship of distributions of pairwise distance values changes depending on whether species or nucleotide *k*-mers are considered. For instance, considering only species content, Bushbuckridge has less beta diversity than Sweden, but this pattern is reversed when considering nucleotide *k*-mer content (Figure 4D). Further, the same observation is true for the relationship between Madagascar and the United States (Figure 4E). Additionally, we compared species and nucleotide beta diversity within each population using Jaccard distance, which is computed based on shared and distinct features irrespective of abundance. In nucleotide *k*-mer space, all nonwestern populations have greater beta diversity than each western population (Figure S10), though this is not the case when only species are considered. This indicates that gut microbiomes in these nonwestern cohorts have a longer "tail" of lowly abundant organisms which differ between individuals.

These observations are critically important to our understanding of beta diversity in the gut microbiome in western and nonwestern communities, as it suggests against the generalization of an inverse relationship between alpha and beta diversity, and in some cases may represent an artifact of limitations in reference databases used for sequence classification.

Improving reference collections via metagenomic assembly

Classification of metagenomic sequencing reads can be improved by assembling sequencing data into metagenomic contigs and grouping these contigs into draft genomes (binning), yielding metagenome-assembled genomes (MAGs). The majority of publications to date have focused on creating MAGs from short-read sequencing data (Almeida et al., 2019; Nayfach et al., 2019; Pasolli et al., 2019), but generation of high-quality MAGs from long-read data from stool samples has been recently reported (Moss et al., 2020). To better characterize the genomes present in our samples, we assembled and binned shotgun sequencing reads from South African samples into MAGs (Figure S11). We generated 3312 MAGs (43 high-quality, 1510 medium-quality, and 1944 low-quality) (Bowers et al., 2017) from 168 metagenomic samples, which yielded a set of 1192 non-redundant medium-quality or better representative strain genomes when filtered for completeness greater than 50%, and contamination less than 10% and de-replicated at 99% average nucleotide identity (ANI). This collection of de-replicated genomes includes VANISH taxa including *Prevotella*, *Treponema*, and *Sphaerochaeta* species (Figure S12, Table S10).

Interestingly, many MAGs within this set represent organisms that are uncommon in Western microbiomes or not easily culturable, including organisms from the genera *Treponema* and *Vibrio*. As short-read MAGs are typically fragmented and exclude mobile genetic elements, we explored methods to create more contiguous genomes, with a goal of trying to better understand these understudied taxa. We performed long-read sequencing on three samples from participants in Bushbuckridge with an Oxford Nanopore MinION sequencer (taxonomic composition of the three samples shown in Figure S13). Samples were chosen for nanopore sequencing on the basis of molecular weight distribution and total mass of DNA (see Methods). One flow cell per sample generated an average 19.71 Gbp of sequencing with a read N50 of 8,275 bp after basecalling. From our three samples, we generated 741 nanopore MAGs (nMAGs), which yielded 35 non-redundant genomes when filtered for completeness greater than 50% and contamination less than 10%, and de-replicated at 99% ANI (Table 2, Figure S11, Table S11). All of the de-replicated nMAGs contained at least one full length 16S sequence, and the contig N50 of 28 nMAGs was greater than 1 Mbp (Table S11).

We compared assembly statistics between all MAGs and nMAGs, and found that while nMAGs were typically evaluated as less complete by CheckM, the contiguity of nanopore medium- and high-quality MAGs was an order of magnitude higher (mean nMAG N50 of 260.5 kb compared to mean N50 of medium- and high-quality MAGs of 15.1 kb) at comparable levels of average coverage (Figure S11, Figure S14). We expect that CheckM under-calculates the completeness of nanopore MAGs due to the homopolymer errors common in nanopore sequencing, which result in frameshift errors when annotating genomes. Indeed, we observe that nanopore MAGs with comparable high assembly size and low contamination to short-read MAGs are evaluated by CheckM as having lower completeness (Figure S14).

Novel genomes generated through nanopore sequencing

When comparing the de-replicated medium- and high-quality nMAGs with the corresponding short-read MAG for the same organism, we find that nMAGs typically include many mobile genetic elements and associated genes that are absent from the short-read MAG, such as transposases, recombinases, phages, and antibiotic resistance genes (Figure 5A).

Additionally, a number of the nMAGs are among the first contiguous genomes in their clade. For example, we assembled two single contig, megabase-scale genomes from the genus *Treponema,* a clade that contains various commensal and pathogenic species and is uncommon in the gut microbiota of western individuals (Obregon-Tito et al., 2015; Schnorr et al., 2014). The first of these genomes is a single-contig *Treponema succinifaciens* genome. The type strain of *T. succinifaciens*, isolated from the swine gut (Han et al., 2011), is the only genome of this species currently available in public reference collections. Our *T. succinifaciens* genome is the first complete genome of this species from the gut of a human. We assembled a second *Treponema* sp. (Figure S15), which contains an aryl polyene biosynthetic gene cluster and shares 92.1% ANI with *T. succinifaciens*. Additionally, we assembled a 5.08 Mbp genome for *Lentisphaerae sp*., which has been shown to be significantly enriched in traditional populations (Angelakis et al., 2019). This genome also contains an aryl polyene biosynthetic gene cluster and multiple beta-lactamases, and shares 94% 16S rRNA identity with *Victivallis vadensis*, suggesting a new species or genus of the family *Victivallaceae* and representing the second closed genome for the phylum *Lentisphaerae*.

Other nMAGs represent organisms that are prevalent in western individuals but challenging to assemble due to their genome structure. Despite the prevalence of *Bacteroides* in western microbiomes, only three closed *B. vulgatus* genomes are available in RefSeq. We assembled a single contig, 2.68 Mbp *Bacteroides vulgatus* genome that is 65.0% complete and 2.7% contaminated and contains at least 16 putative insertion sequences, which may contribute to the lack of contiguous short-read assemblies for this species. Similarly, we assembled a single-contig genome for *Catabacter sp.*, a member of the order *Clostridiales*; the most contiguous *Catabacter* genome in GenBank is in five scaffolded contigs (Parks et al., 2017). The putative *Catabacter sp.* shares 85% ANI with the best match in GenBank, suggesting that it represents a new species within the *Catabacter* genus or a new genus entirely, and it contains a sactipeptide biosynthetic gene cluster. Additionally, we assembled a 3.6 Mbp genome for *Prevotella sp.* (N50 = 1.87 Mbp), a highly variable genus that is prevalent in nonwestern microbiomes and associated with a range of effects on host health (Scher et al., 2013). Notably, the first closed genomes of *P. copri*, a common species of *Prevotella*, were only recently assembled with nanopore sequencing of metagenomic samples; one from a human stool sample (Moss et al., 2020) and the other from cow rumen (Stewart et al., 2019). *P. copri* had previously evaded closed assembly from short-read sequence data due to the dozens of repetitive insertion sequences within its genome (Moss et al., 2020). Notably, this *Prevotella* assembly contains cephalosporin and beta-lactam resistance genes, as well as an aryl polyene biosynthetic gene cluster.

We observed that many long-read assembled genomes were evaluated to be of low completeness despite having contig N50 values greater than 1 Mbp. In investigating this phenomenon, we discovered that many of these genomes had sparse or uneven short-read coverage, leading to gaps in short-read polishing that would otherwise correct small frameshift errors. To polish genomic regions that were not covered with short-reads, we performed long-read polishing on assembled contigs from each sample, and re-binned polished contigs. Long-read polishing improved the completeness of many organisms that are not commonly described in the gut microbiota, due perhaps to their low relative abundance in the average human gut, or to biases in shotgun sequencing library preparation that limit their detection (Figure S16, Figure S17). For example, we generated a 2 Mbp genome that is best classified as a species of the phylum Melainabacteria. Melainabacteria is a non-photosynthetic phylum closely related to Cyanobacteria that has been previously described in the gut microbiome and is associated with consuming a vegetarian diet (Di Rienzi et al., 2013). Melainabacteria have proven difficult to isolate and culture, and the only complete, single-scaffold genome existing in RefSeq was assembled from shotgun sequencing of a human fecal sample (Di Rienzi et al., 2013). Interestingly, our Melainabacteria genome has a GC content of 30.9%, and along with assemblies of a *Mycoplasma sp.* (25.3% GC) and *Mollicutes sp.* (28.1% GC) (Figure S18)*,* represent AT-rich organisms that can be underrepresented in shotgun sequencing data due to the inherent GC bias of transposon insertion and amplification-based sequencing approaches (Sato et al., 2019) (Figure S17). Altogether, these three genomes increased in completeness by an average of 28.5% with long-read polishing to reach an overall average of 70.9% complete. While these genomes meet the accepted standards to be considered medium-quality, it is possible that some or all of these highly contiguous, megabase scale assemblies are complete or near-complete yet underestimated by CheckM due to incomplete polishing.

Altogether, we find that *de novo* assembly approaches are capable of generating contiguous, high-quality assemblies for novel organisms, offering potential for investigation into the previously unclassified matter in the microbiomes of these nonwestern communities. In particular, nanopore sequencing was able to produce contiguous genomes for organisms that are difficult to assemble due to repeat structures (*Prevotella sp.*, *Bacteroides vulgatus*), as well as for organisms that exist on the extreme ends of the GC content spectrum (*Mollicutes sp.*, *Melainabacteria sp.*). We observe that long-reads are able to capture a broader range of taxa both at the read and assembly levels when compared to short-read assemblies, and that short- and long-read polishing approaches are able to yield medium-quality or greater draft genomes for these organisms. This illustrates the increased visibility that *de novo* assembly approaches lend to the study of the full array of organisms in the gut microbiome.

Discussion

Together with Oduaran *et al.* (Oduaran et al., 2020), we provide the first description of gut microbiome composition in Soweto and Bushbuckridge, South Africa, and to our knowledge, the first effort utilizing shotgun and nanopore sequencing in South Africa to describe the gut microbiome of adults. In doing so, we increase global representation in microbiome research and provide a baseline for future studies of disease association with the microbiome in South African populations, and in other transitional populations.

We find that gut microbiome composition differs demonstrably between the Bushbuckridge and Soweto cohorts, further highlighting the importance of studying diverse communities with differing lifestyle practices. Interestingly, even though gut microbiomes of individuals in Bushbuckridge and Soweto share many features and are more similar to each other than to other global cohorts studied, we do observe hallmark taxa associated with westernization are enriched in microbiomes in Soweto. These include *Bacteroides* and *Bifidobacterium*, which have been previously associated with urban communities (Gupta et al., 2017), consistent with Soweto's urban locale in the Johannesburg metropolitan area.

We also observe enrichment in relative abundance of crAssphage and crAss-like viruses in Soweto relative to Bushbuckridge, with relatively high prevalence in both cohorts yet lower abundance on average of crAssphage clades alpha and delta compared to several other populations. This furthers recent work which revealed that crAssphage is prevalent across many cohorts globally (Edwards et al., 2019), but found relatively fewer crAssphage sequences on the African continent, presumably due to paucity of available shotgun metagenomic data. Just as shotgun metagenomic sequence data enables the study of viruses, it also enables us to assess the relative abundance of human cells or damaged human cells in the stool. Surprisingly, we observe a high relative abundance of human DNA in the raw sequencing data, which was unexpected. We find a statistically significantly higher relative abundance of human DNA in samples from Soweto compared to those from Bushbuckridge. Future research may help illuminate the potential reason for this finding, which may include a higher proportion of epithelium disrupting, invasive bacteria or parasites in Soweto vs. Bushbuckridge, and in South Africa, in general, compared to other geographic settings. Alternatively, this may also be attributable to a higher baseline of intestinal inflammation and fecal shedding of leukocytes. Without additional information, it is difficult to speculate as to the reason for this finding.

We find that individuals in Bushbuckridge are enriched in VANISH taxa including *Succinatimonas*, which has been recently reported to associate with microbiomes from individuals practicing traditional lifestyles (Pasolli et al., 2019). Intriguingly, several VANISH taxa (*Succinatimonas*, *Succinivibrio*, *Treponema*) display bimodal distributions in the Bushbuckridge cohort. We hypothesize that this bimodality could be caused by differences in lifestyle and/or environmental factors including diet, history of hospitalization or exposure to medicines, physical properties of the household dwelling, differential treatment of drinking water across the villages comprising Bushbuckridge. Additionally this pattern may be explained by participation in migration to and from urban centers (or sharing a household with a migratory worker). A higher proportion of men in the community engage in this pattern of rural-urban migration (Ginsburg et al., 2016), but it is possible that sharing a household with a cyclical worker could influence gut microbiome composition via horizontal transmission (Brito et al., 2019).

Despite the fact that host genetics explain relatively little of the variation in microbiome composition (Rothschild et al., 2018), we do observe a small number of taxa that associate with host genetics in this population. Future work is required for replication and to determine whether these organisms are interacting with the host and whether they are associated with host health.

Additionally, we demonstrate marked differences between South African cohorts and other previously studied populations living on the African continent and western countries. Broadly, we find that South African microbiomes reflect the transitional nature of their communities in that they overlap with western and nonwestern populations. Tremendous human genetic diversity exists within Africa, and our work reveals that there is a great deal of as yet unexplored microbiome diversity as well. In fact, we find that microbiome beta diversity within communities may be systematically underestimated by incomplete reference databases: taxa that are unique to individuals in nonwestern populations are not present in reference databases and therefore not included in beta diversity calculations. Though it has been reported that nonwestern and traditional populations tend to have higher alpha diversity but lower beta diversity compared to western populations, we show that this pattern is not universally upheld when reference-agnostic nucleotide comparisons are performed. By extension, we speculate that previous claims that beta diversity inversely correlates with alpha diversity may have been fundamentally limited by study design in some cases. Specifically, the disparity between comparing small, homogenous African populations with large, heterogenous western ones constitutes a significant statistical confounder, potentially preventing a valid assessment of beta diversity between groups. Furthermore, alpha and beta diversity comparisons based on species-level taxonomic assignment may be further confounded due to the presence of polyphyletic clades in organisms like *Prevotella copri* (Parks et al., 2020; Tett et al., 2019) which are highly abundant in gut microbiomes of nonwestern individuals.

Through a combination of short-read and long-read sequencing, we successfully assembled contiguous, complete genomes for many organisms that are underrepresented in reference databases, including genomes that are commonly considered to be enriched in or limited to populations with traditional lifestyles including members of the VANISH taxa (e.g., *Treponema sp., Treponema succinifaciens*). The phylum *Spirochaetes*, namely its constituent genus *Treponema*, is considered to be a marker of traditional microbiomes and has not been detected in high abundance in human microbiomes outside of those communities (Angelakis et al., 2019; Obregon-Tito et al., 2015). Here, we identify *Spirochaetes* in the gut microbiome of individuals in urban Soweto, demonstrating that this taxon is not exclusive to traditional, rural populations, though we observe that relative abundance is higher on average in traditional populations. Generation of additional genomes of VANISH taxa and incorporation of these genomes into reference databases will allow for increased sensitivity to detect these organisms in metagenomic data. Additionally, these genomes facilitate comparative genomics of understudied gut microbes and allow for functional annotation of potentially biologically relevant functional pathways. We note that many of these genomes (e.g., Melainabacteria, *Succinatimonas*) are enriched in the gut microbiota of Bushbuckridge participants relative to Soweto, highlighting the impact of metagenomic assembly to better resolve genomes present in rural populations.

We produced genomes for organisms that exist on the extremes of the GC content spectrum, such as *Mycoplasma sp.*, *Mollicutes sp.*, and *Melainabacteria sp*. We find that these organisms are sparsely covered by short-read sequencing, illustrating the increased range of non-amplification based sequencing approaches, such as nanopore sequencing. Interestingly, these assemblies are evaluated as only medium-quality by CheckM despite having low measurements of contamination, as well as genome lengths and gene counts comparable to reference genomes from the same phylogenetic clade. We hypothesize that sparse short-read coverage leads to incomplete polishing and therefore retention of small frameshift errors, which are a known limitation of nanopore sequencing (Tyler et al., 2018). Further evaluation of 16S or long-read sequencing of traditional and western populations can identify whether these organisms are specific to certain lifestyles, or more prevalent but poorly detected with shotgun sequencing.

While we find that the gut microbiome composition of the two South African cohorts described herein reflects their lifestyle transition, we acknowledge that these cohorts are not necessarily representative of all transitional communities in South Africa or other parts of the world which differ in lifestyle, diet, and resource access. Hence, further work remains to describe the gut microbiota in detail of other such understudied populations. This includes a detailed characterization of parasites present in microbiome sequence data, an analysis that we did not undertake in this study but would be of great interest. These organisms have been detected in the majority of household toilets in nearby KwaZulu-Natal province (Trönnberg et al., 2010), and may interact with and influence microbiota composition (Leung et al., 2018).

Our study has several limitations. Although the publicly available sequence data from other global cohorts were generated with similar methodology to our study, it is possible that batch effects exist between datasets generated in different laboratories that may explain some percentage of the global variation we observe. Additionally, while nanopore sequencing is able to broaden our range of investigation, we illustrate that our ability to produce well-polished genomes at GC content extremes is limited. This may affect our ability to accurately call gene lengths and structures, although iterative long-read polishing improves our confidence in these assemblies. Future investigation of these communities using less biased, higher coverage short-read approaches or more accurate long-read sequencing approaches, such as PacBio circular consensus sequencing, may improve assembly qualities. Additionally, long-read sequencing of samples from a wider range of populations can identify whether the genomes identified herein are limited to traditional and transitional populations, or more widespread. Further, future improvements in error rate of long-read sequencing may obviate the need for short-read polishing altogether.

Taken together, our results emphasize the importance of generating sequence data from diverse transitional populations to contextualize studies of health and disease in these individuals. To do so with maximum sensitivity and precision, reference genomes must be generated to classify sequencing reads from these metagenomes. Herein, we demonstrate the discrepancies in microbiome sequence classifiability across global populations and highlight the need for more comprehensive reference collections. Recent efforts have made tremendous progress in improving the ability to classify microbiome data through creating new genomes via metagenomic assembly (Almeida et al., 2019; Nayfach et al., 2019; Pasolli et al., 2019), and here we demonstrate the application of short- and long-read metagenomic assembly techniques to create additional genome references. Our application of long-read sequencing technology to samples from South African individuals has demonstrated the ability to generate highly contiguous MAGs and shows immense potential to expand our reference collections and better describe microbiomes throughout diverse populations globally. In the future, microbiome studies may utilize a combination of short- and long-read sequencing to maximize information output, perhaps performing targeted Nanopore sequencing of samples that are likely to contain the most novelty on the basis of short-read data.

The present study was conducted in close collaboration between site staff and researchers in Bushbuckridge and Soweto as well as microbiome experts both in South Africa and the United States, and community member feedback was considered at multiple phases in the planning and execution of the study (see Oduaran *et al.* 2020 for more information). Tremendous research efforts have produced detailed demographic and health characterization of individuals living in both Bushbuckridge and Soweto (Kabudula et al., 2017a, 2017b; Ramsay et al., 2016; Richter et al., 2007) and it is our hope that microbiome data can be incorporated into this knowledge framework in future studies to uncover disease biomarkers or microbial associations with other health and lifestyle outcomes. More broadly, we feel that this is an example of a framework for conducting microbiome studies in an equitable manner, and we envision a system in which future studies of microbiome composition can be carried out to achieve detailed characterization of microbiomes globally while maximizing benefit to all participants and researchers involved.

Methods

Cohort selection

Stool samples were collected from women aged 40-72 years in Soweto, South Africa and Bushbuckridge Municipality, South Africa. Participants were recruited on the basis of participation in AWI-Gen (Ramsay et al., 2016), a previous study in which genotype and extensive health and lifestyle survey data were collected. Human subjects research approval was obtained (Stanford IRB 43069, University of the Witwatersrand Human Research Ethics Committee M160121, Mpumalanga Provincial Health Research Committee MP_2017RP22_851) and informed consent was obtained from participants for all samples collected. Stool samples were collected and preserved in OmniGene Gut OMR-200 collection kits (DNA Genotek). Samples were frozen within 60 days of collection as per manufacturer's instructions, followed by long-term storage at -80°C. As the enrollment criteria for our study included previous participation in a larger human genomics project (Ramsay et al., 2016), we had access to self-reported ethnicity for each participant (BaPedi, Ndebele, Sotho, Tsonga, Tswana, Venda, Xhosa, Zulu, Other, or Unknown). Samples from participants who tested HIV-positive or who did not consent to an HIV test were not analyzed.

Metagenomic sequencing of stool samples

DNA was extracted from stool samples using the QIAamp PowerFecal DNA Kit (QIAGEN) according to the manufacturer’s instructions except for the lysis step, in which samples were lysed using the TissueLyser LT (QIAGEN) (30 second oscillations/3 minutes at 30Hz). DNA concentration of all DNA samples was measured using Qubit Fluorometric Quantitation (DS DNA High-Sensitivity Kit, Life Technologies). DNA sequencing libraries were prepared using the Nextera XT DNA Library Prep Kit (Illumina). Final library concentration was measured using Qubit Fluorometric Quantitation and library size distributions were analyzed with the Bioanalyzer 2100 (Agilent). Libraries were multiplexed and 150 base pair paired-end reads were generated on the HiSeq 4000 platform (Illumina). Samples with greater than approximately 300 ng remaining mass and a peak fragment length of greater than 19,000 bp (with minimal mass under 4,000 bp) as determined by a TapeStation 2200 (Agilent Technologies, Santa Clara, CA) were selected for nanopore sequencing. Nanopore sequencing libraries were prepared using the 1D Genomic DNA by Ligation protocol (ONT, Oxford UK) following standard instructions. Each library was sequenced with a full FLO-MIN106D R9 Version Rev D flow cell on a MinION sequencer for at least 60 hours.

Computational methods

R code for analysis and figure generation will be made available on Github upon publication.

Preprocessing

Stool metagenomic sequencing reads were trimmed using TrimGalore v0.5.0 (Krueger), a wrapper for CutAdapt v1.18 (Martin, 2011), with a minimum quality score of 30 for trimming (--q 30) and minimum read length of 60 (--length 60). Trimmed reads were deduplicated to remove PCR and optical duplicates using seqtk rmdup v1.3-r106 with default parameters. Reads aligning to the human genome (hg19) were removed using BWA v0.7.17-r1188 (Li and Durbin, 2009). To assess the microbial composition of our short-read sequencing samples, we used the Kraken v2.0.8-beta taxonomic sequence classifier with default parameters (Wood and Salzberg, 2014) and a comprehensive custom reference database containing all bacterial and archaeal genomes in GenBank assembled to “complete genome,” “chromosome,” or “scaffold” quality as of January 2020. Bracken v2.0.0 was then used to re-estimate abundance at each taxonomic rank (Lu et al., 2017).

Additional data

Published data from additional populations were downloaded via the NCBI Sequence Read Archive (SRA) or European Nucleotide Archive (Table S9) and preprocessed and taxonomically classified as described above. For datasets containing longitudinal samples from the same individual, one unique sample per individual was chosen (the first sample from each individual was chosen from the United States Human Microbiome Project cohort).

K-mer sketches

K-mer sketches were computed using sourmash v2.0.0 (Brown and Irber, 2016). Low abundance *k*-mers were trimmed using the “trim-low-abund.py” script from the khmer package (Crusoe et al., 2015) with a *k*-mer abundance cutoff of 3 (-C 3) and trimming coverage of 18 (-Z 18). Signatures were computed for each sample using the command “sourmash compute” with a compression ratio of 1000 (--scaled 1000) and *k*-mer lengths of 21, 31, and 51 (-k 21,31,51). Two signatures were computed for each sample - one signature tracking *k*-mer abundance (--

track-abundance flag) for angular distance comparisons, and one without this flag for Jaccard distance comparisons. Signatures at each length of *k* were compared using "sourmash compare" with default parameters and the correct length of *k* specified with the -k flag.

Statistical analysis and plotting

Statistical analyses were performed using R v4.0.0 (R Core Team, 2019) with packages MASS v7.3-51.5 (Venables and Ripley, 2002), stats (R Core Team, 2019), ggsignif v0.6.0 (Ahlmann-Eltze, 2019), and ggpubr v0.2.5 (Kassambara, 2020). Alpha and beta diversity were calculated using the vegan package v2.5-6 (Oksanen et al., 2019). Wilcoxon rank-sum tests were used to compare alpha and beta diversity between cohorts. Count data were normalized via cumulative sum scaling and log2 transformation (Paulson et al., 2013) prior to MDS. Data separation in MDS was assessed via PERMANOVA (permutation test with pseudo F ratios) using the adonis function from the vegan package. Differential microbial features between individuals living in Soweto and Bushbuckridge were identified from unnormalized count data output from kraken2 classification and bracken abundance re-estimation and filtered for 20% prevalence and at least 1000 sequencing reads using DESeq2 (Love et al., 2014). Plots were generated in R using the following packages: cowplot v1.0.0 (Wilke, 2019), DESeq2 v1.24.0 (Love et al., 2014), dplyr v0.8.5 (Wickham et al., 2020), genefilter v1.66.0 (Gentleman et al., 2019), ggplot2 v3.3.0 (Wickham, 2016), ggpubr v0.2.5, ggrepel v0.8.2 (Slowikowski, 2020), ggsignif v0.6.0, gtools v3.8.2 (Warnes et al., 2020), harrietr v0.2.3 (Gonçalves da Silva, 2017), MASS v7.3-51.5, reshape2 v1.4.3 (Wickham, 2007), and vegan v2.5-6.

Genome assembly, binning, and evaluation

Short-read metagenomic data were assembled with MEGAHIT v1.1.3 (Li et al., 2016) and binned into draft genomes as previously described (Bishara et al., 2018). Briefly, short reads were aligned to assembled contigs with BWA v0.7.17 (Li and Durbin, 2009) and contigs were subsequently binned into draft genomes with MetaBAT v2:2.13 (Kang et al., 2015). Bins were evaluated for size, contiguity, completeness, and contamination with QUAST v5.0.0 (Gurevich et al., 2013), CheckM v1.0.13 (Parks et al., 2015), Prokka v1.13 (Seemann, 2014), Aragorn v1.2.38 (Laslett and Canback, 2004), and Barrnap v0.9 (https://github.com/tseemann/barrnap/). We referred to published guidelines to designate genome quality (Bowers et al., 2017). Individual contigs from all assemblies were assigned taxonomic classifications with Kraken v2.0.8 (Bowers et al., 2017; Wood and Salzberg, 2014). Genome sets were filtered for completeness greater than 50% and contamination less than 10% as evaluated by CheckM, and de-replicated using dRep v2.5.4 (Olm et al., 2017) with ANI threshold to form secondary clusters (-sa) at 0.99 (strain-level) or 0.95 (species-level).

Long-read data were assembled with Lathe (Moss et al., 2020) as previously described. Briefly, Lathe implements basecalling with Guppy v2.3.5, assembly with Flye v2.4.2 (Lin et al., 2016), short-read polishing with Pilon v1.23 (Walker et al., 2014), and circularization with Circlator (Hunt et al., 2015) and Encircle (Moss et al., 2020). Binning, classification, and de-replication were performed as described above. Additional long-read polishing was performed using four iterations of polishing with Racon v1.4.10 (Vaser et al., 2017) and long-read alignment using minimap2 v2.17-r941 (Li, 2018), followed by one round of polishing with Medaka v0.11.5 (https://github.com/nanoporetech/medaka).

Direct comparisons between nMAGs and corresponding MAGs were performed by de-replicating high- and medium-quality nMAGs with MAGs assembled from the same sample. MAGs sharing at least 99% ANI with an nMAG were aligned to the nMAG regions using nucmer v3.1 and uncovered regions of the nMAG were annotated with prokka 1.14.6, VIBRANT v1.2.1, and ResFams v1.2. Taxonomic trees were plotted with Graphlan v1.1.3 (Asnicar et al., 2015).

To construct phylogenetic trees, reference 16S sequences were downloaded from the Ribosomal Database Project (Release 11, update 5, September 30, 2016) (Cole et al., 2014) and 16S sequences were identified from nanopore genome assemblies using Barrnap v0.9 (https://github.com/tseemann/barrnap/). Sequences were aligned with MUSCLE v3.8.1551 (Edgar, 2004) with default parameters. Maximum-likelihood phylogenetic trees were constructed from the alignments with FastTree v2.1.10 (Edgar, 2004; Price et al., 2010) with default settings (Jukes-Cantor + CAT model). Support values for branch splits were calculated using the Shimodaira-Hasegawa test with 1,000 resamples (default). Trees were visualized with FigTree v1.4.4 (http://tree.bio.ed.ac.uk/software/figtree/).

Data availability

All shotgun sequence data generated by this study, as well as metagenome-assembled genome sequences, will be deposited in a publicly available reference database (NCBI Sequence Read Archive or European Nucleotide Archive) and released upon publication.

Participant-level metadata (age, BMI, blood pressure measurements, and concomitant medications) and human genetic data will be deposited in the European Genome-phenome Archive and released upon publication.

Acknowledgements

We thank the participants in our study for taking part in this research. Additionally, we thank the Bushbuckridge Community Advisory Group for their thoughtful recommendations on study procedure. We thank Karen Andrade for her contributions in planning the 2019 Community Advisory Group workshop. We thank the INDEPTH consortium for their support of this project. We thank the numerous fieldworkers at the Soweto DPHRU and Agincourt HDSS who enrolled participants and collected data. In particular, we thank Melody Mabuza, the field worker at Agincourt HDSS who oversaw collection of Bushbuckridge participant enrollment, and Jackson Mabasa, who managed sample collection in Soweto. We thank Michèle Ramsay (AWI-Gen PI), Yusuf Ismail, and Amanda Haye for their contributions to organizational and sample processing aspects of the project. We thank the Stanford Research Computing Center and Ben Siranosian for their contributions to computational infrastructure and support.

Funding

This work was supported in part by a grant from the Stanford Center for Innovation in Global Health and by NIH grant P30 CA124435, which supports the following Stanford Cancer Institute Shared Resource: the Genetics Bioinformatics Service Center. A.S.B was supported by the Rosenkranz prize and by an R01 AI148623 from the National Institute of Allergy and Infectious Diseases. F.B.T. was supported by the National Science Foundation Graduate Research Fellowship and the Stanford Computational, Evolutionary, and Human Genetics Pre-Doctoral Fellowship. D.G.M was supported by the Stanford Graduate Fellowships in Science and Engineering program. O.H.O. was partially supported by a Fogarty Global Health Equity Scholar award (TW009338). ANW is supported by the Fogarty International Centre, National Institutes of Health under award number K43TW010698. The work was further supported by the South African National Research Foundation (CPRR160421162721) and a seed grant from the African Partnership for Disease Control. The AWI-Gen project is supported by the National Human Genome Research Institute (U54HG006938) as part of the H3A Consortium. The MRC/Wits Rural Public Health and Health Transitions Research Unit and Agincourt Health and

Socio-Demographic Surveillance System, a node of the South African Population Research Infrastructure Network (SAPRIN), is supported by the Department of Science and Innovation, the University of the Witwatersrand and the Medical Research Council, South Africa, and previously the Wellcome Trust, UK (grants 058893/Z/99/A; 069683/Z/02/Z; 085477/Z/08/Z; 085477/B/08/Z).This paper describes the views of the authors and does not necessarily represent the official views of the National Institutes of Health (USA).

Main Tables

Table 1. Participant characteristics

	Site	Mean	Standard deviation	Range
Age	**Bushbuckridge**	55.52	7.79	43 - 72
	Soweto	54.1	5.86	43 - 64
BMI	**Bushbuckridge**	32.35	8.00	21.2 - 59*
	Soweto	36.05	9.25	20.42 - 58.62
Systolic blood pressure	**Bushbuckridge**	137	18.28	101 - 189
	Soweto	134	22.54	96 - 193
Diastolic blood pressure	**Bushbuckridge**	84	12.12	54 - 119
	Soweto	90	14.37	58 - 119

*One participant's BMI measurement was excluded on the basis of the recorded value being too low to be physiologically possible and deemed to have been recorded in error. We could not validate the correct BMI for this participant and thus have omitted them from the BMI summary statistics.

Table 2. Medium- and high-quality genomes assembled from nanopore sequencing

Classification	Size (Mb)	% GC	N50 (Mb)	Quality	16S	Antibiotic Resistance Genes	Phages	Transposases	Biosynthetic Gene Clusters	Polishing
Alistipes putredinis	1.91	53.1	1.91	Medium	2	1	1	1	0	Short
Anaerotruncus sp.	2.04	43.7	2.04	Medium	2	2	2	4	1	Short
Bacilli bacterium	1.46	26.2	1.46	Medium	1	0	2	1	1	Short
Bacteroidales bacterium	2.67	47.3	1.80	High	3	0	4	16	0	Short
Bacteroidales bacterium	2.79	49.8	2.79	High	4	3	0	29	0	Short
Bacteroidales bacterium	1.7	56.6	1.70	Medium	1	1	0	6	0	Short
Bacteroides sp.	2	48.2	1.59	High	3	1	0	7	0	Short
Bacteroides sp.	2.82	43.3	2.00	Medium	6	1	3	31	0	Short
Bacteroides vulgatus	2.68	42.7	2.68	Medium	3	0	0	14	0	Short
Candidatus Melainabacteria	2	30.9	2.00	Medium	1	0	4	0	0	Long and Short
Catabacter sp.	1.65	46.4	1.65	Medium	1	2	1	0	1	Long and Short
Clostridiales bacterium	2.03	57.9	0.60	Medium	4	2	2	6	1	Short
Clostridiales bacterium	1.53	47.3	1.53	Medium	1	1	1	1	1	Short
Clostridiales bacterium	1.95	49.6	0.73	Medium	3	5	2	1	1	Short
Clostridiales bacterium	2.24	48.7	0.58	Medium	2	3	3	12	1	Short
Clostridiales bacterium	2.65	42.8	2.65	Medium	3	0	3	6	2	Short
Clostridiales bacterium	1.32	45.2	0.79	Medium	1	3	2	4	1	Short
Clostridiales bacterium	1.61	46.9	1.61	Medium	1	1	2	0	0	Short
Clostridium sp.	1.53	25.2	1.53	Medium	1	0	2	1	0	Short
Clostridium sp.	1.3	46.9	1.30	Medium	1	2	1	0	0	Short
Clostridium sp.	2.01	28.8	2.01	Medium	3	2	3	3	0	Short
Clostridium sp.	1.14	29.1	1.14	Medium	1	0	1	0	0	Short
Clostridium sp.	2.44	52.5	2.23	High	3	6	3	1	3	Short
Eubacterium	2	44.5	0.63	Medium	2	1	1	5	0	Short
Lachnospiraceae bacterium	3.38	43.6	1.94	Medium	4	7	2	10	0	Short
Lachnospiraceae bacterium	3.81	43.6	2.83	Medium	4	6	2	28	2	Short
Lentisphaeria bacterium	5.08	57.5	5.08	Medium	3	3	4	84	1	Long and Short
Mollicutes bacterium	1.68	28.1	1.49	Medium	2	1	1	2	0	Long and Short
Mycoplasma sp.	1.17	25.3	1.12	Medium	2	2	0	1	0	Long and Short
Oscillibacter sp.	1.13	57.4	0.17	Medium	1	0	2	2	0	Short
Porphyromonadaceae bacterium	2.97	47.4	2.97	Medium	5	1	1	9	0	Short
Prevotella sp.	3.29	43.6	1.14	Medium	6	3	2	17	1	Long and Short
Ruminococcaceae bacterium	1.95	38.4	0.80	Medium	4	0	1	8	0	Short
Ruminococcaceae bacterium	2.27	51.4	2.27	High	3	4	2	4	1	Short
Ruminococcaceae bacterium	1.78	58.3	1.78	Medium	3	3	0	9	0	Short
Treponema sp.	2.06	41.6	2.06	Medium	3	0	2	2	1	Short
Treponema succinifaciens	2.55	39.1	2.55	High	4	0	0	15	0	Short
uncultured Ruminococcus	1.59	44.0	1.34	Medium	2	2	0	2	1	Short
uncultured Ruminococcus	2.08	46.9	2.08	Medium	5	2	6	8	1	Short

Figures

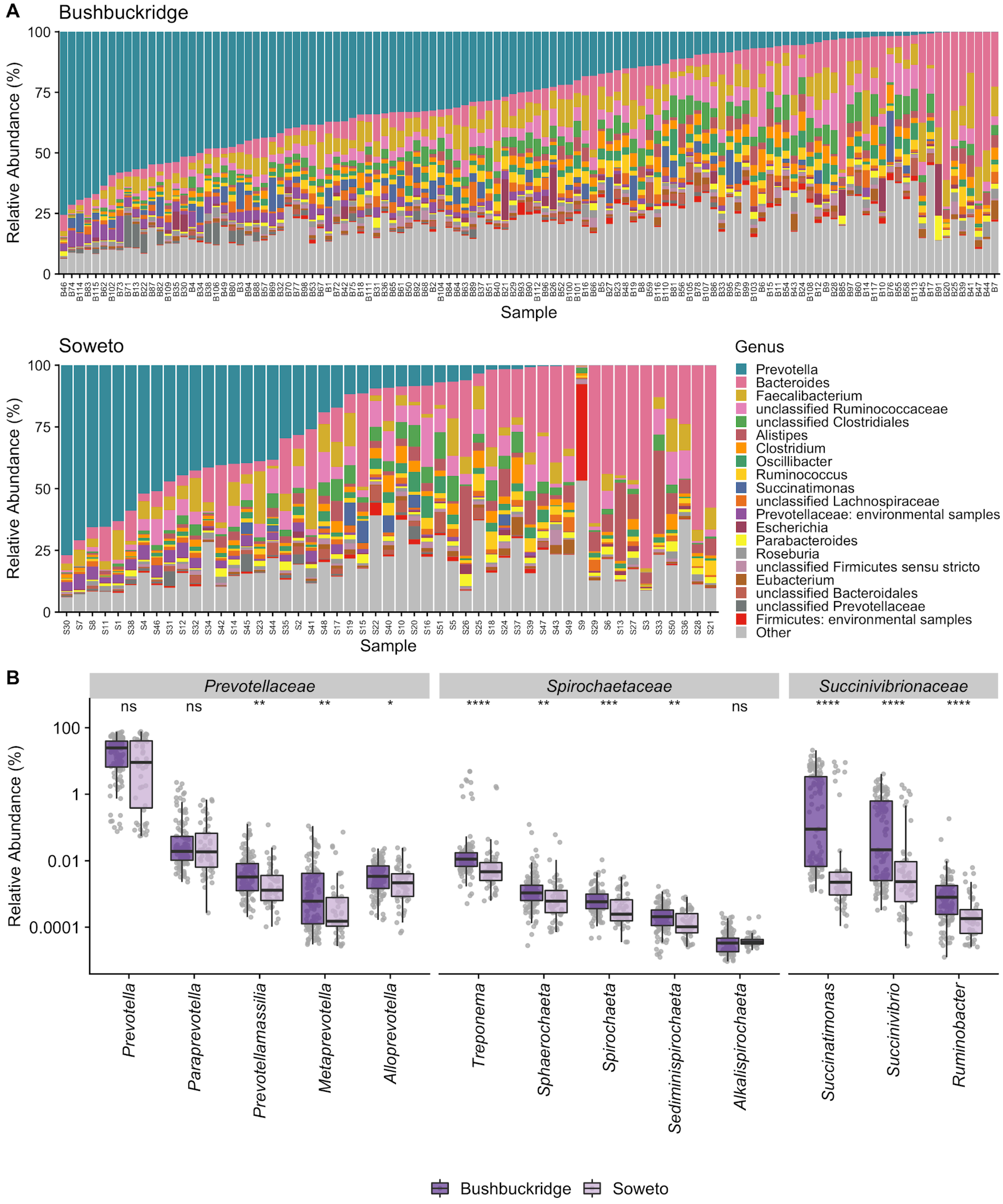

Figure 1. Taxonomic composition of South African study participants

Sequence data were taxonomically classified using Kraken2 with a database containing all genomes in GenBank of scaffold quality or better as of January 2020.

(A) Top 20 genera by relative abundance for samples from participants in Bushbuckridge and Soweto, sorted by decreasing *Prevotella* abundance. *Prevotella*, *Faecalibacterium*, and *Bacteroides* are the most prevalent genera across both study sites.

(B) Relative abundance of VANISH genera by study site, grouped by family. A pseudocount of 1 read was added to each sample prior to relative abundance normalization in order to plot on a log scale, as the abundance of some genera in some samples is zero. Relative abundance values of most VANISH genera are higher on average in participants from Bushbuckridge than Soweto (Wilcoxon rank-sum test, significance values denoted as follows: (*) $p < 0.05$, (**) $p < 0.01$, (***) $p < 0.001$, (****) $p < 0.0001$, (ns) not significant). Upper and lower box plot whiskers represent the highest and lowest values within 1.5 times the interquartile range, respectively.

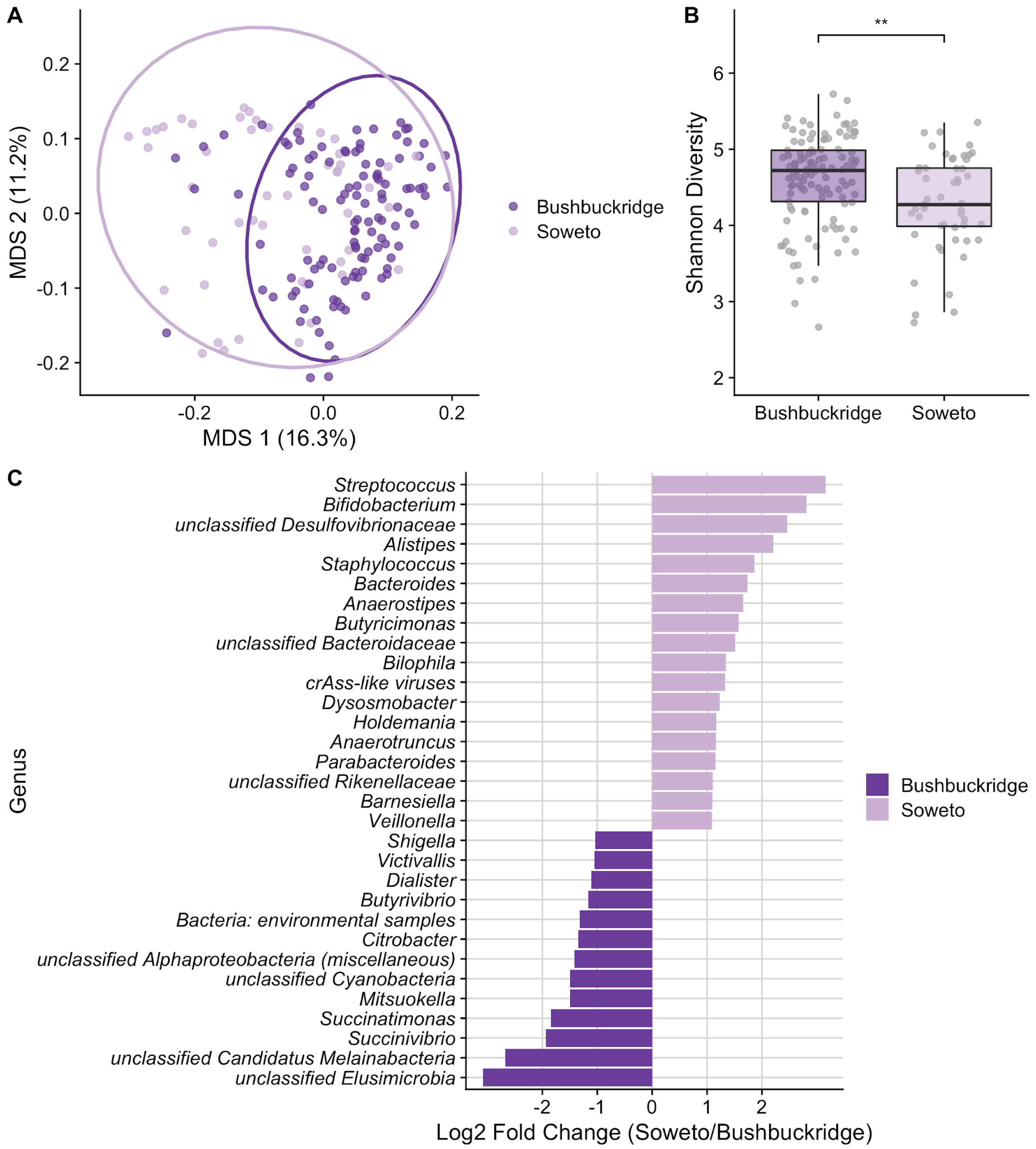

Figure 2. Comparison of Bushbuckridge and Soweto microbiomes

(A) Multidimensional scaling of pairwise Bray-Curtis distance between samples (CSS-normalized counts). Samples from Soweto have greater dispersion than samples from Bushbuckridge (PERMDISP2 $p < 0.001$).

(B) Shannon diversity calculated on species-level taxonomic classifications for each sample. Samples from Bushbuckridge are higher in alpha diversity than samples from Soweto (Wilcoxon rank-sum test, $p < 0.001$). Upper and lower box plot whiskers represent the highest and lowest values within 1.5 times the interquartile range, respectively.

(C) DESeq2 identifies microbial genera that are differentially abundant in rural Bushbuckridge compared to the urban Soweto cohort. Features with log2 fold change greater than one are plotted (full results in Table S7).

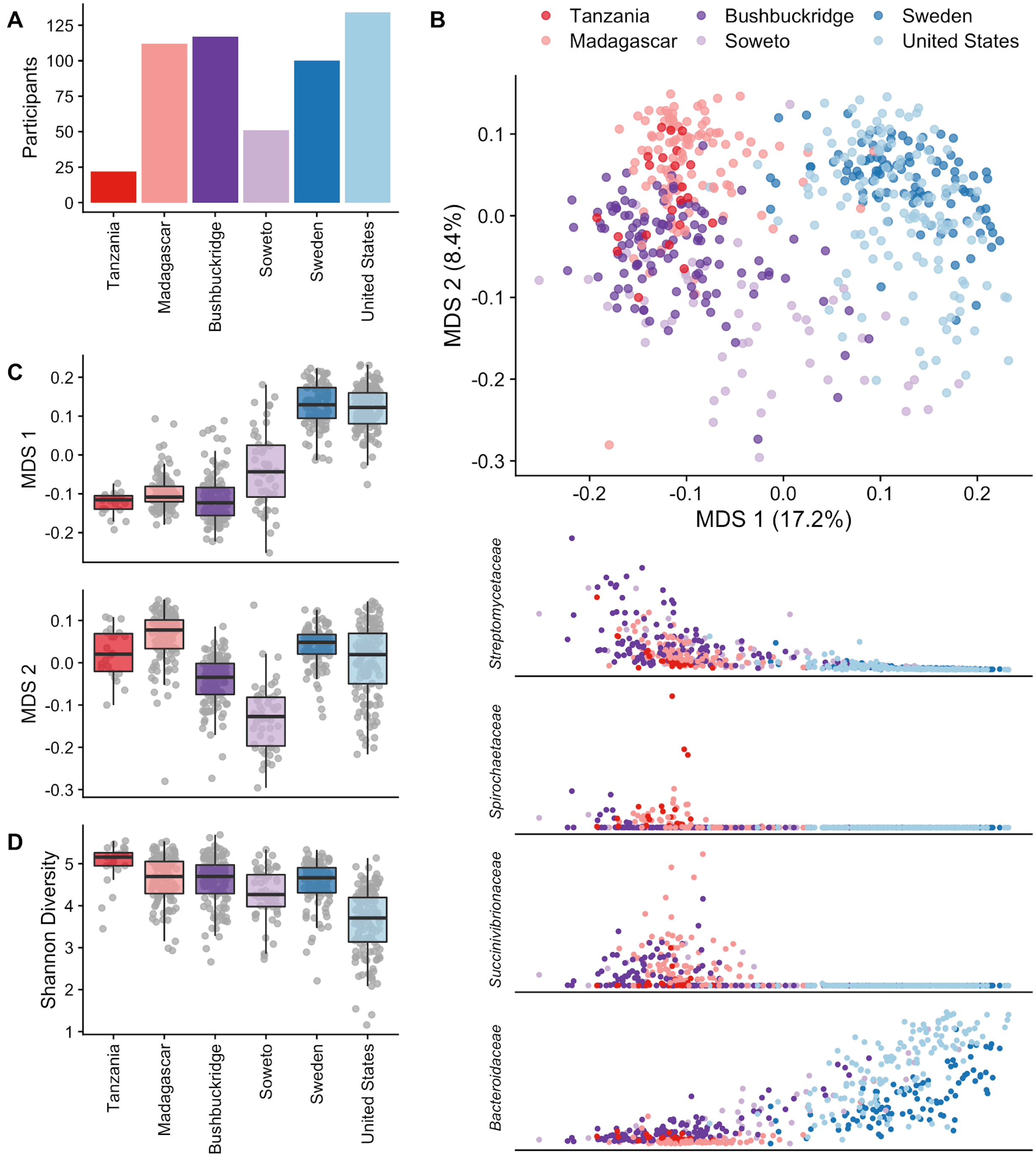

Figure 3. Community-level comparison of global microbiomes

Comparisons of South African microbiome data to microbiome sequence data from four publicly available cohorts representing western (United States, Sweden) and nonwestern (Hadza hunter-gatherers of Tanzania, rural Madagascar) populations.

(A) Number of participants per cohort.

(B) Multidimensional scaling of pairwise Bray-Curtis distance between samples from six datasets of healthy adult shotgun microbiome sequencing data. Western populations (Sweden, United States) cluster away from African populations practicing a traditional lifestyle (Madagascar, Tanzania) while transitional South African microbiomes overlap with both western and nonwestern populations. Shown below are scatterplots of relative abundance of the top four taxa most correlated with MDS 1 (Spearman's rho, *Streptomycetaceae* 0.853, *Spirochaetaceae* 0.850, *Succinivibrionaceae* 0.845, *Bacteroidaceae* -0.801) against MDS 1 on the x axis.

(C) Boxplot of the first axis of MDS (MDS 1) which correlates with geography and lifestyle, and the second axis of MDS (MDS 2) where South African populations display a shift relative to other cohorts.

(D) Shannon diversity across cohorts. Shannon diversity was calculated from data rarefied to the number of sequence reads of the lowest sample.

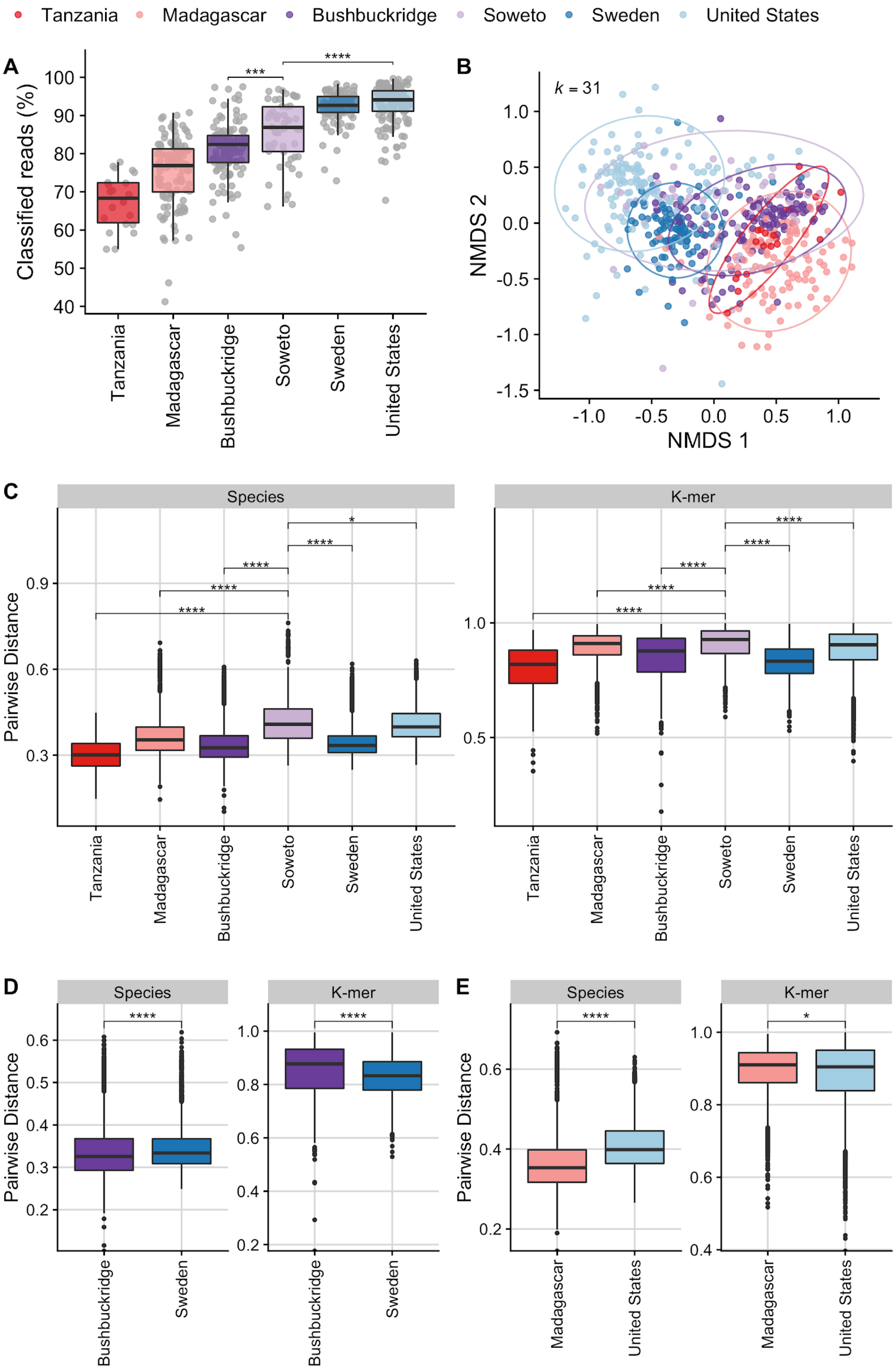
● Tanzania
● Madagascar
● Bushbuckridge
● Soweto
● Sweden
● United States
A
Classified reads (%)
100
90
80
70
60
50
40
***
****
Tanzania
Madagascar
Bushbuckridge
Soweto
Sweden
United States
B
k = 31
NMDS 2
NMDS 1
1.0
0.5
0.0
-0.5
-1.0
-1.5
-1.0
-0.5
0.0
0.5
1.0
C
Species
K-mer
Pairwise Distance
0.9
0.6
0.3
1.0
0.5
****
*
D
Species
K-mer
Pairwise Distance
0.6
0.5
0.4
0.3
0.2
1.0
0.8
0.6
0.4
0.2
Bushbuckridge
Sweden
E
Species
K-mer
Pairwise Distance
0.6
0.4
0.2
1.0
0.8
0.6
0.4
Madagascar
United States

Figure 4. Comparison of beta diversity between communities calculated by taxonomy versus nucleotide *k*-mer composition

(A) Percentage of reads classified at any taxonomic rank, by cohort, based on a reference database of all scaffold or higher quality reference genomes in GenBank and RefSeq as of January 2020. Western microbiomes have a higher percentage of classifiable reads compared to nonwestern microbiomes (Wilcoxon rank-sum test $p < 0.001$).

(B) Nucleotide sequences of microbiome sequencing reads were compared using *k*-mer sketches. This reference-free approach is not constrained by comparison to existing genomes and therefore allows direct comparison of sequences. Briefly, a hash function generates signatures at varying sequence lengths (*k*) and *k*-mer sketches can be compared between samples. Data shown here are generated from comparisons at *k*=31 (approx. species-level)(Koslicki and Falush, 2016). Non-metric multidimensional scaling (NMDS) of angular distance values computed between each pair of samples.

(C-E) Comparison of pairwise beta diversity within communities assessed by Bray-Curtis distance based on species-level classifications and angular distance of nucleotide *k*-mer sketches. (C) All populations. (D) South African populations (Bushbuckridge and Soweto) compared to the Swedish cohort. Beta diversity measured by Bray-Curtis distance is higher in Soweto but lower in Bushbuckridge compared to the United States. However, reference-independent *k*-mer comparisons indicate that nucleotide dissimilarity is higher within both South African populations compared to the Swedish cohort. (E) Species-based Bray-Curtis distance indicates that there is more beta diversity within the United States cohort compared to Malagasy, but *k*-mer distance indicates an opposite pattern.

Significance values for Wilcoxon rank sum tests denoted as follows: (*) $p < 0.05$, (**) $p < 0.01$, (***) $p < 0.001$, (****) $p < 0.0001$.

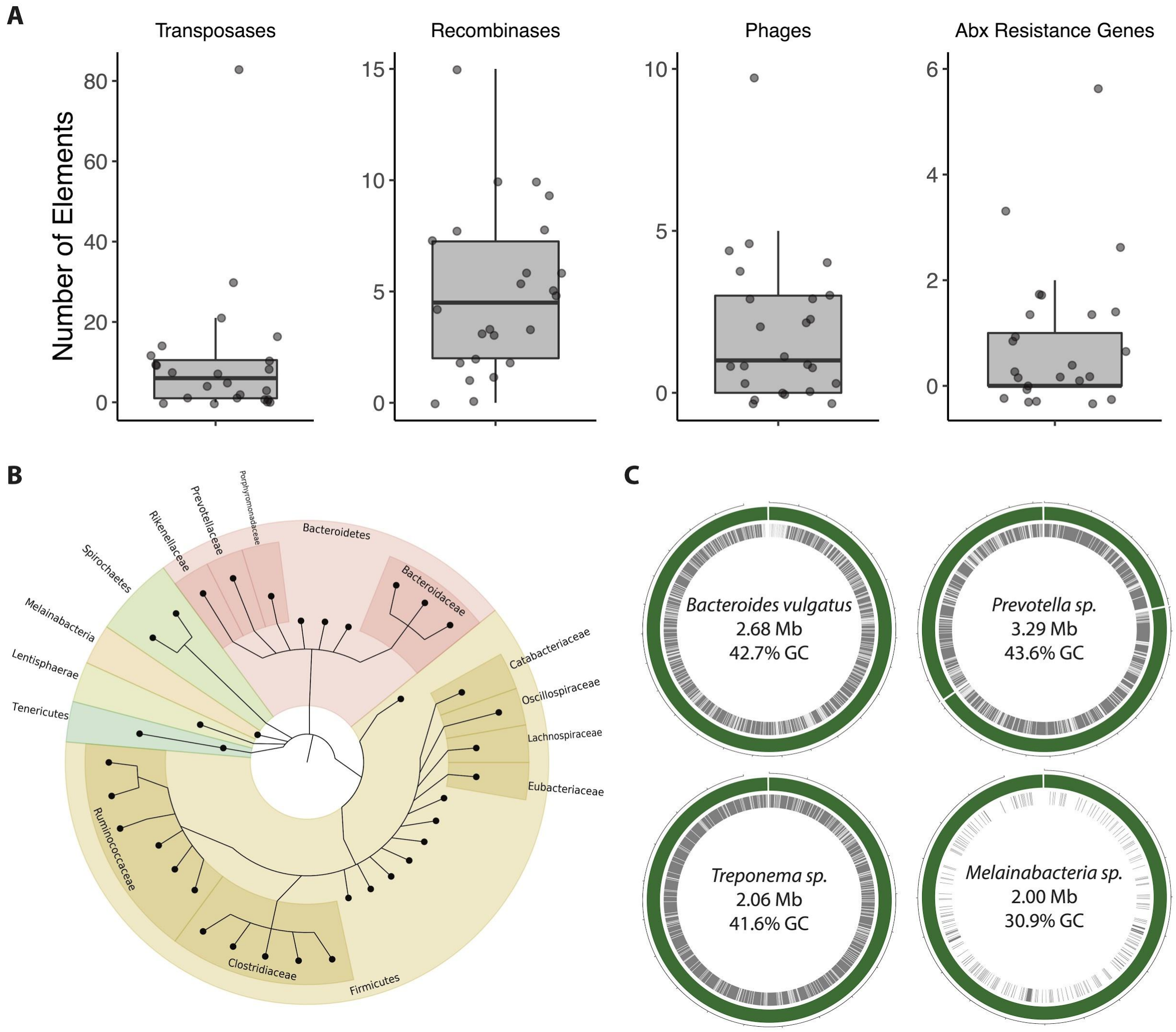

Figure 5. Complete and contiguous genomes of South African microbiota

(A) Number of genomic elements present in medium- and high-quality nanopore MAGs that are absent in corresponding short-read MAGs for the same organism.

(B) Taxonomic classification of de-replicated medium- and high-quality nanopore MAGs. Larger circles represent nanopore MAGs, at the highest level of taxonomic classification.

(C) A selection of MAGs assembled from long-read sequencing (green) of three South African samples compared contigs assembled from corresponding short read data (grey). Outer light grey ring indicates contig scale, with ticks at 100kb intervals. Breaks in circles represent different contigs.

Supplementary Figures

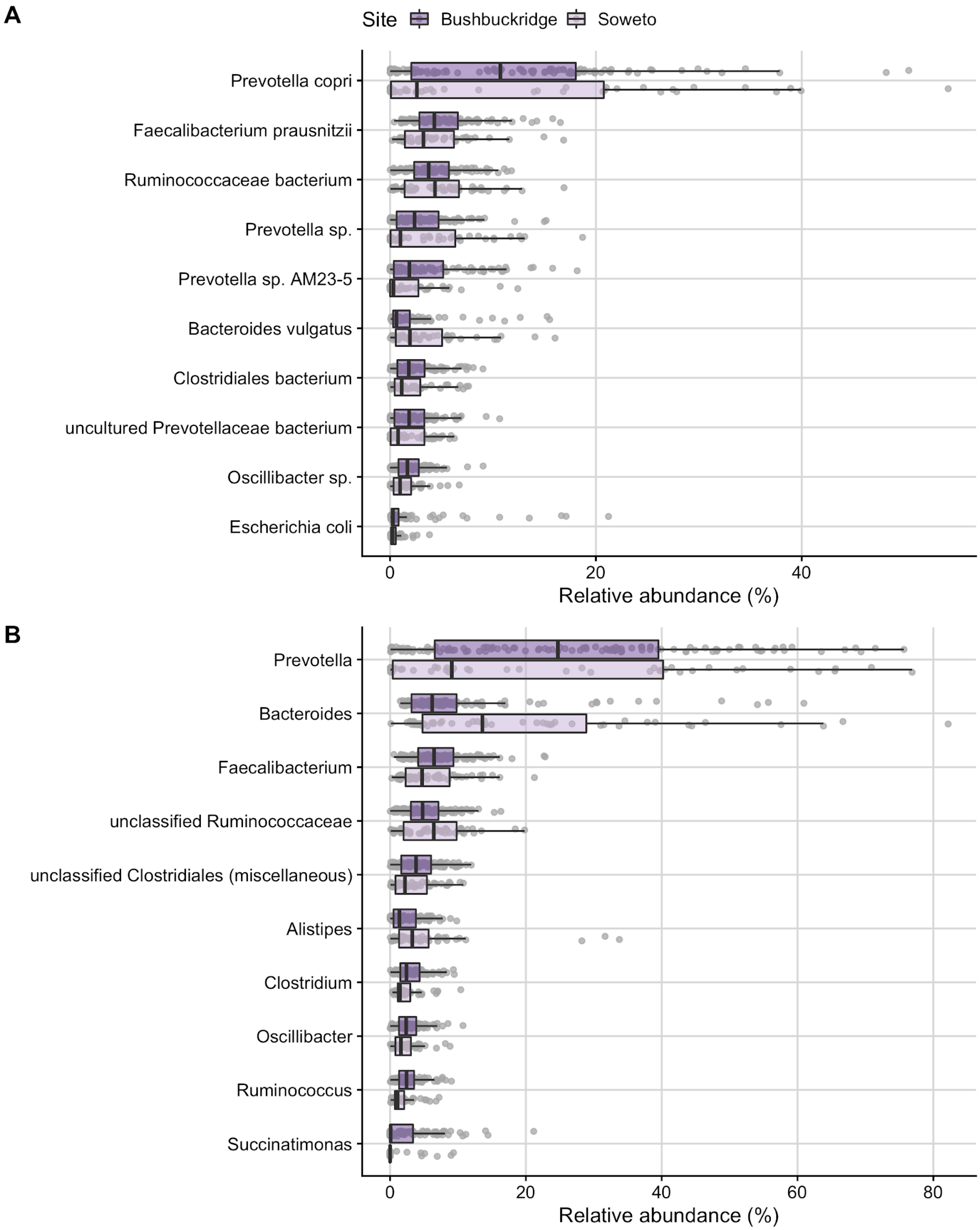

Supplementary Figure 1. Most abundant species and genera

Most abundant taxa by mean relative abundance (total sum scaling) shown for samples from Bushbuckridge (n=117) and Soweto (n=51). Taxa are plotted in decreasing order of mean relative abundance calculated across both cohorts combined. Upper and lower box plot whiskers represent the highest and lowest values within 1.5 times the interquartile range, respectively.

(A) The most abundant species are *Prevotella copri*, *Faecalibacterium prausnitzii,* and a bacterium from the family Ruminococcaceae.

(B) *Prevotella*, *Bacteroides,* and *Faecalibacterium* are the most abundant genera across both study sites.

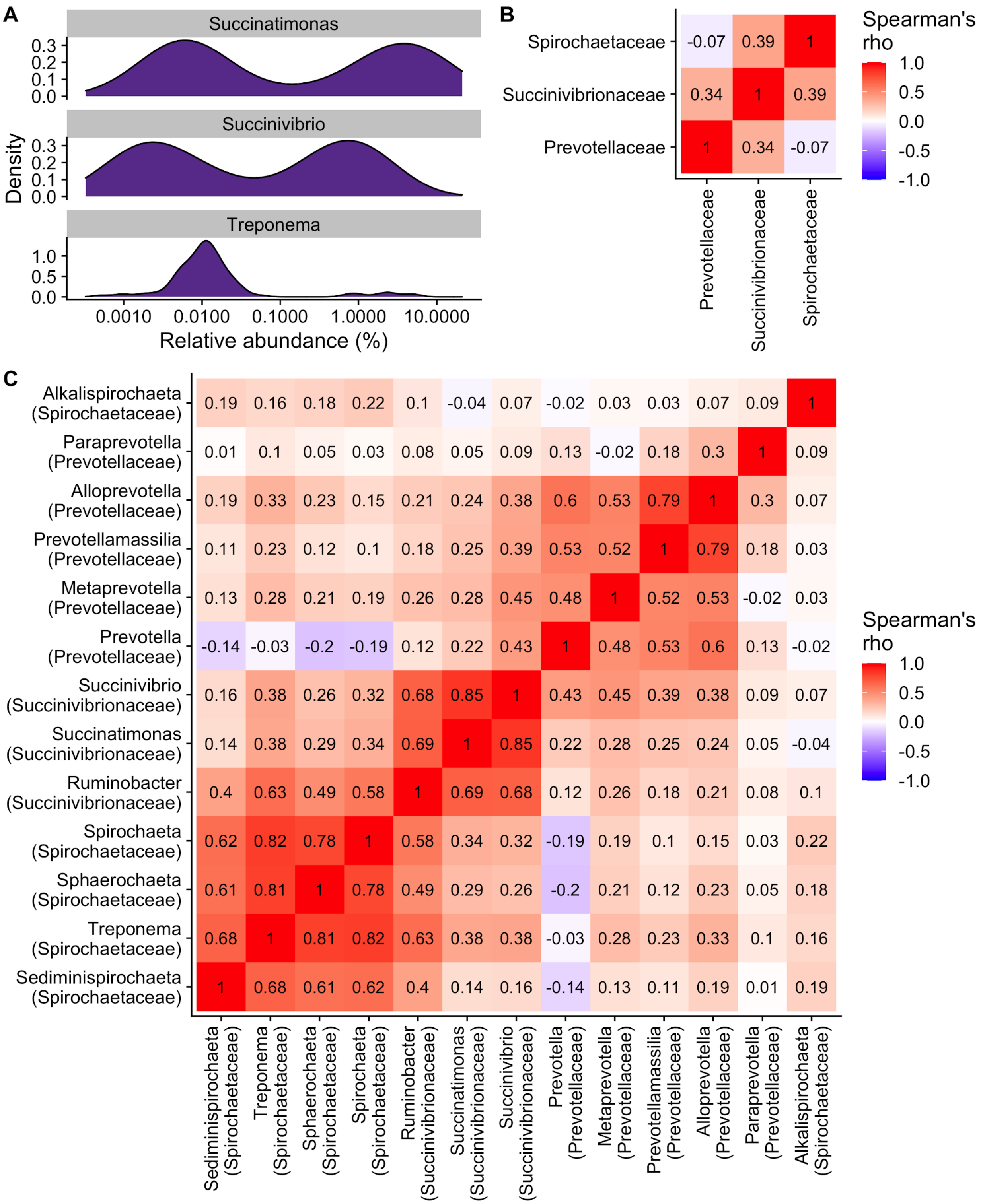

Supplementary Figure 2. Bimodal distribution of three VANISH taxa

(A) *Succinatimonas, Succinivibrio*, and *Treponema* relative abundance values follow a bimodal distribution in Bushbuckridge.

Across all South African samples, several VANISH families (B) and genera (C) are correlated, with the exception of *Prevotella* and genera of the family *Spirochaetaceae* which are not correlated with *Prevotella* (*Treponema*) or weakly anti-correlated with *Prevotella* (*Spirochaeta*, *Sphaerochaeta*, *Sediminispirochaeta*).

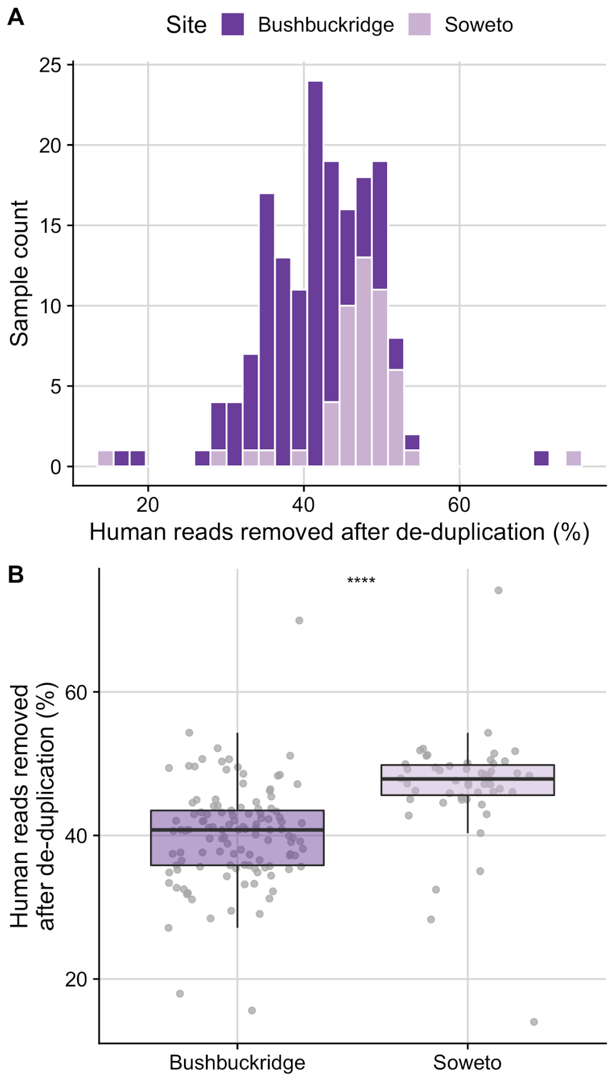

Supplementary Figure 3. Abundance of human reads in metagenomic sequencing

(A) Histogram and (B) box and whisker plots indicating that the proportion of human reads removed after deduplication was found to be higher in the Soweto cohort compared to Bushbuckridge.

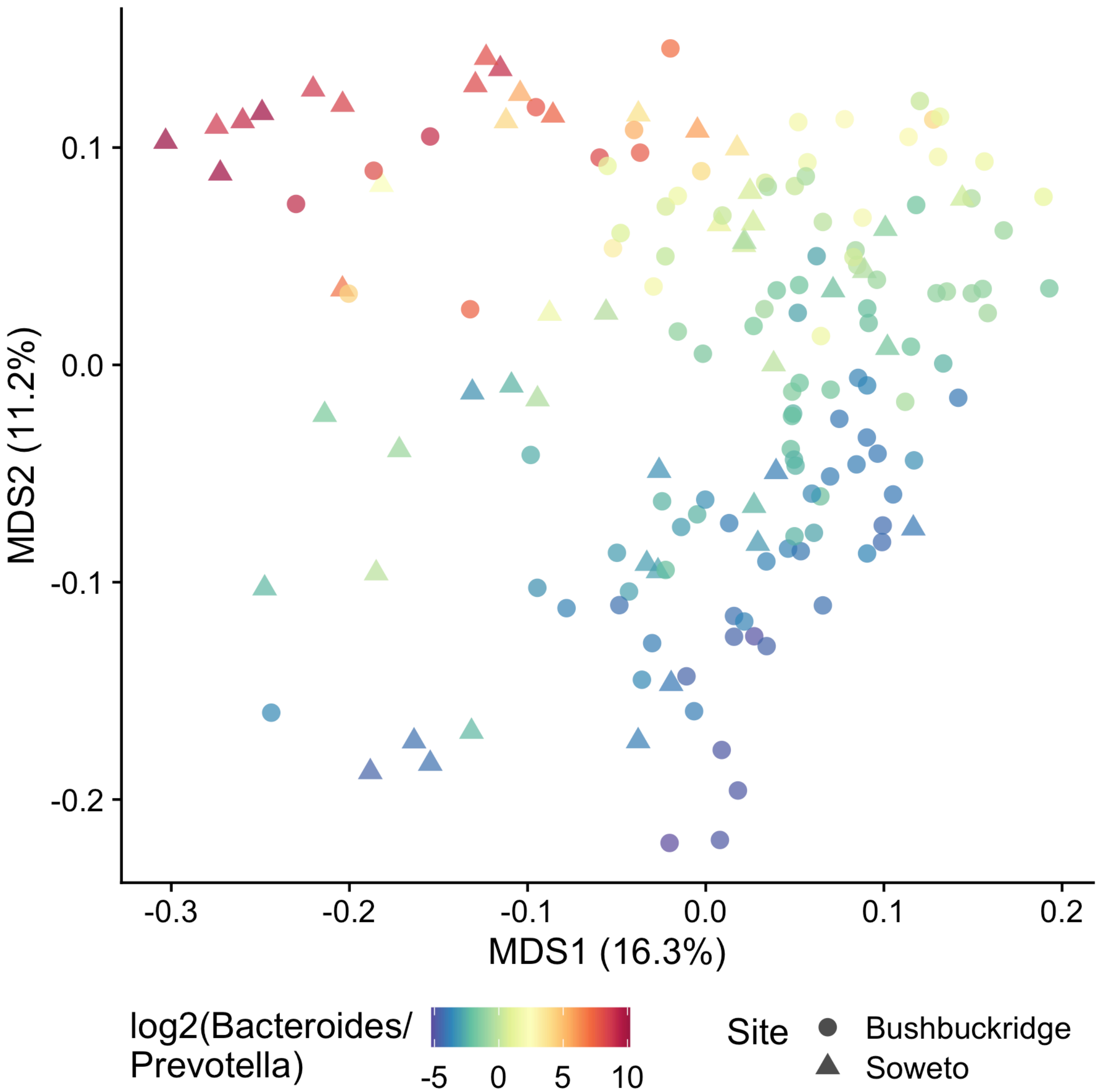

Supplementary Figure 4. Bacteroides/Prevotella gradient across study population

Multidimensional scaling ordination of Bray-Curtis distance calculated from species classifications in South African microbiome samples colored by log2 ratio of the relative abundance of the genera *Bacteroides Prevotella*. *Bacteroides* and *Prevotella* are major axes of variation across study samples.

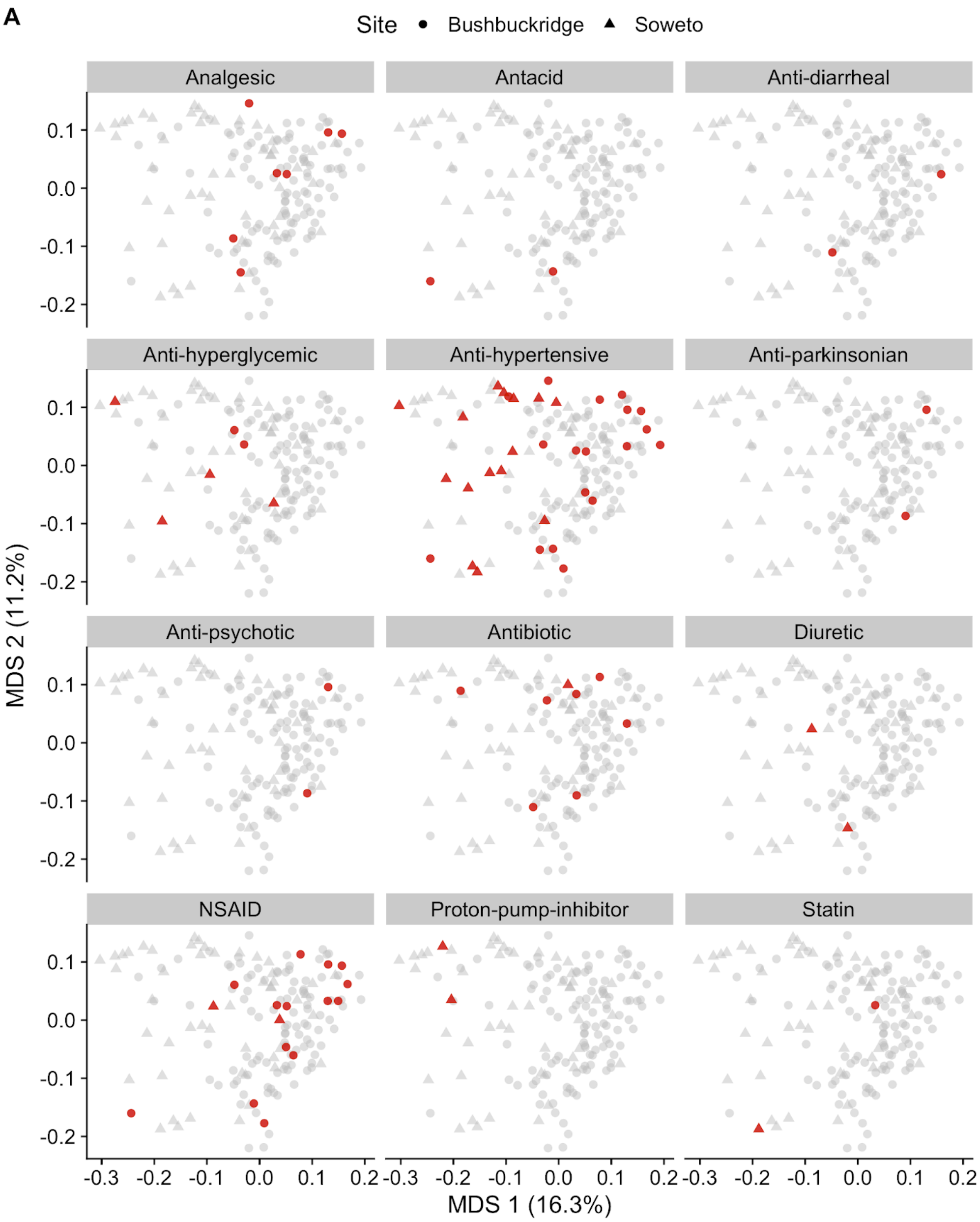

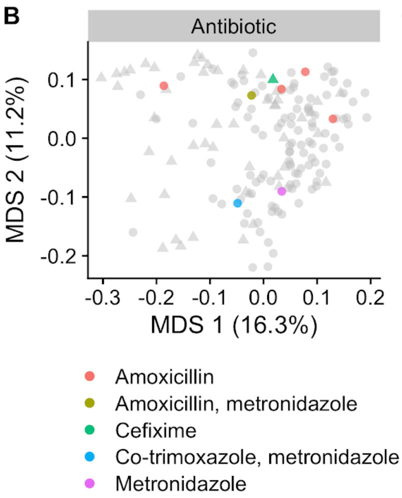

C

Category	R2	Pr(>F)
Analgesic	0.0054	0.504
Antacid	0.0053	0.459
Anti-diarrheal	0.0050	0.555
Anti-hyperglycemic	0.0096	0.070
Anti-hypertensive	0.0048	0.738
Anti-parkinsonian	0.0044	0.725
Anti-psychotic	0.0044	0.736
Antibiotic	0.0045	0.814
Diuretic	0.0059	0.381
NSAID	0.0065	0.318
Proton-pump-inhibitor	0.0136	0.026
Statin	0.0056	0.411

Supplementary Figure 5: Concomitant medications do not substantially impact community composition

Multidimensional scaling ordination of Bray-Curtis distance calculated from species classifications. Circles indicate participants from Bushbuckridge, triangles indicate participants from Soweto.

(A) Points are colored red if the participant was taking a medication of the corresponding class, patients not taking a medication of that class are shown in gray.

(B) Specific antibiotics taken by participants. Points are colored according to the antibiotic or combination of antibiotics reported.

(C) PERMANOVA R^2 values and p-values for the variation explained by each drug class.

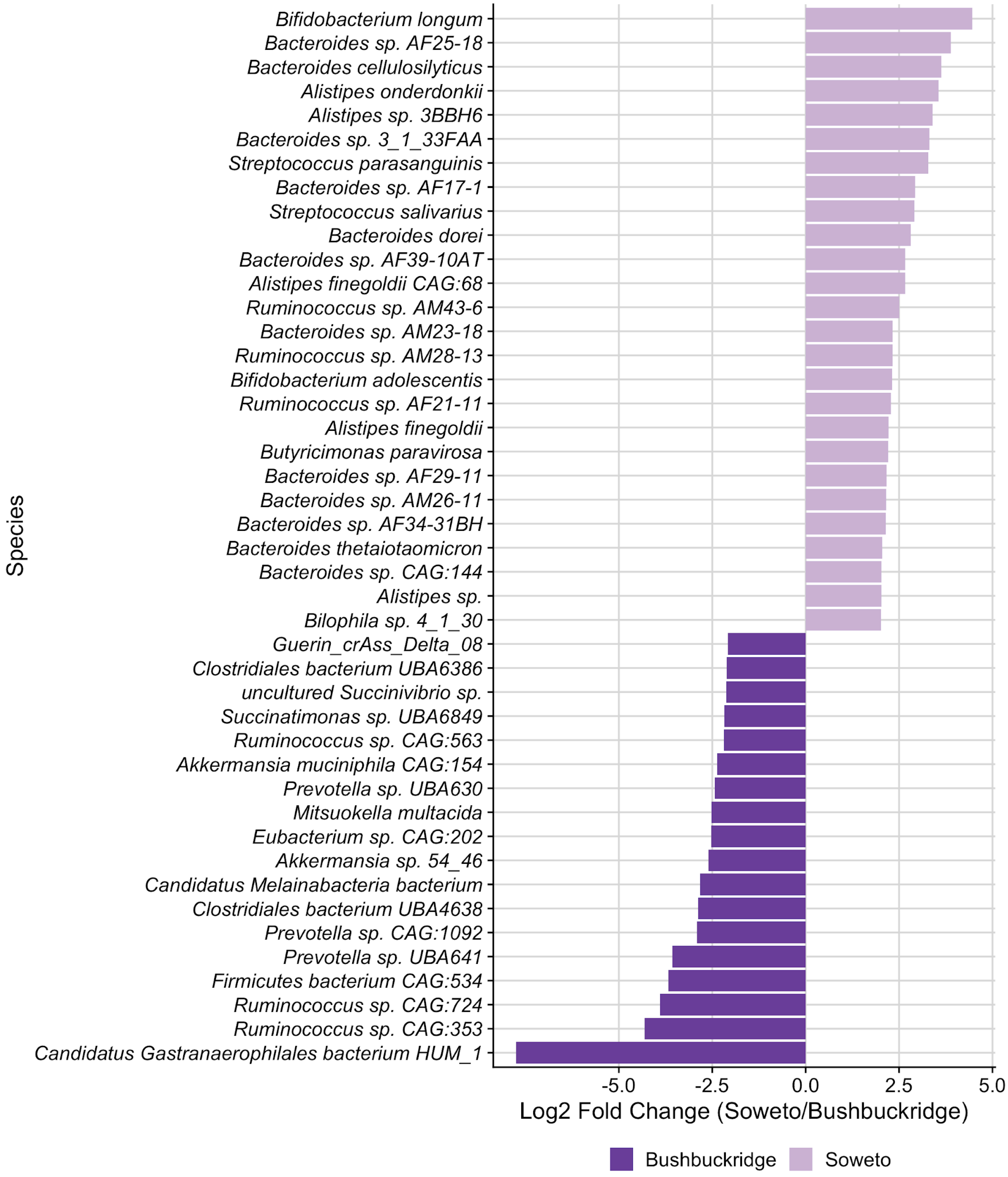

Supplementary Figure 6. Differentially abundant species between Bushbuckridge and Soweto

Differentially abundant microbial species between rural Bushbuckridge and urban Soweto samples identified by DESeq2. Features with log2 fold change greater than one are shown (full results in Table S7). Note that differentially abundant microbial genera are presented in Figure 2c.

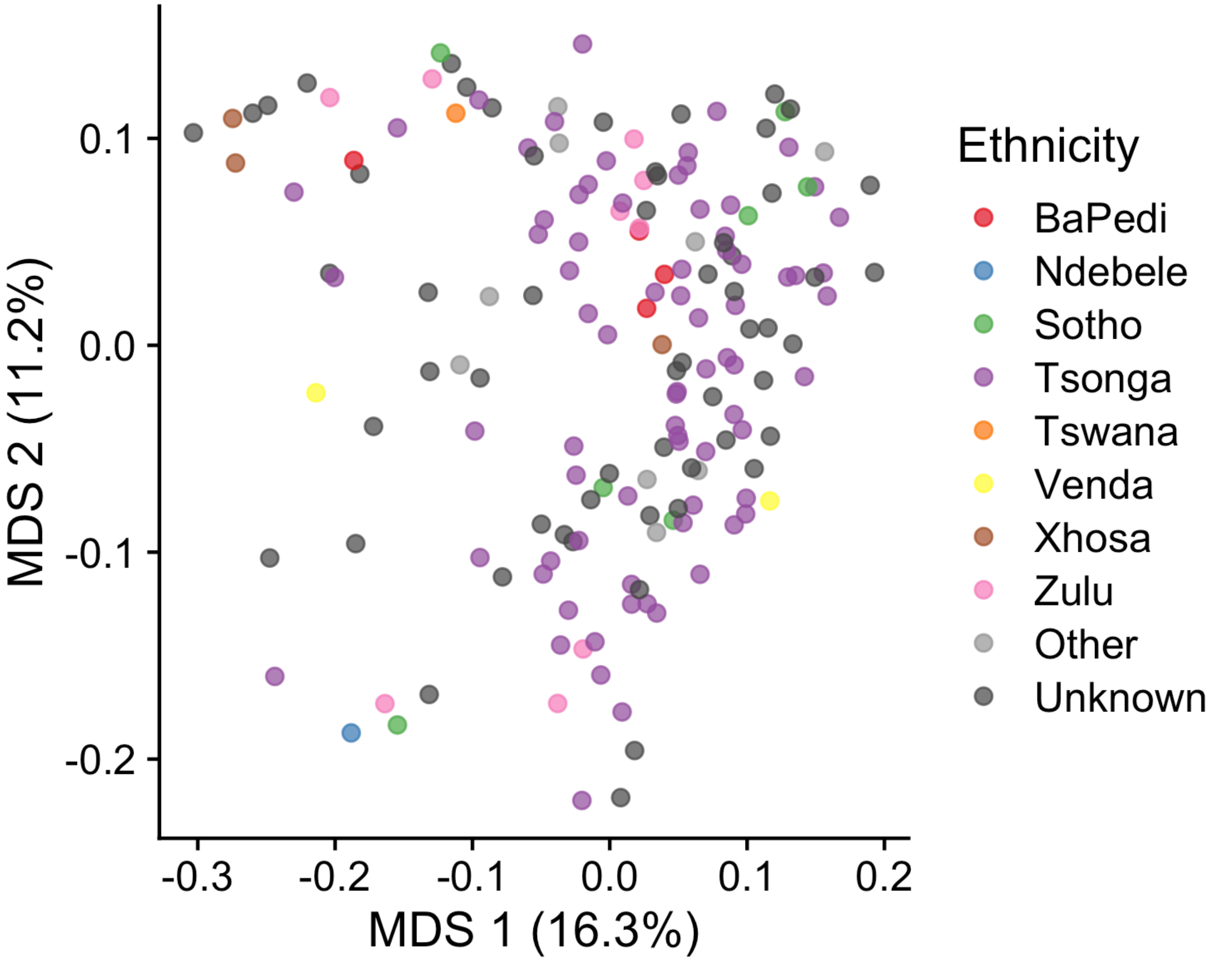

Supplementary Figure 7. South African microbiomes do not cluster by self-reported ethnicity

Multidimensional scaling ordination of Bray-Curtis distance with samples are colored by self-reported ethnicity. Samples do not cluster by self-reported ethnicity.

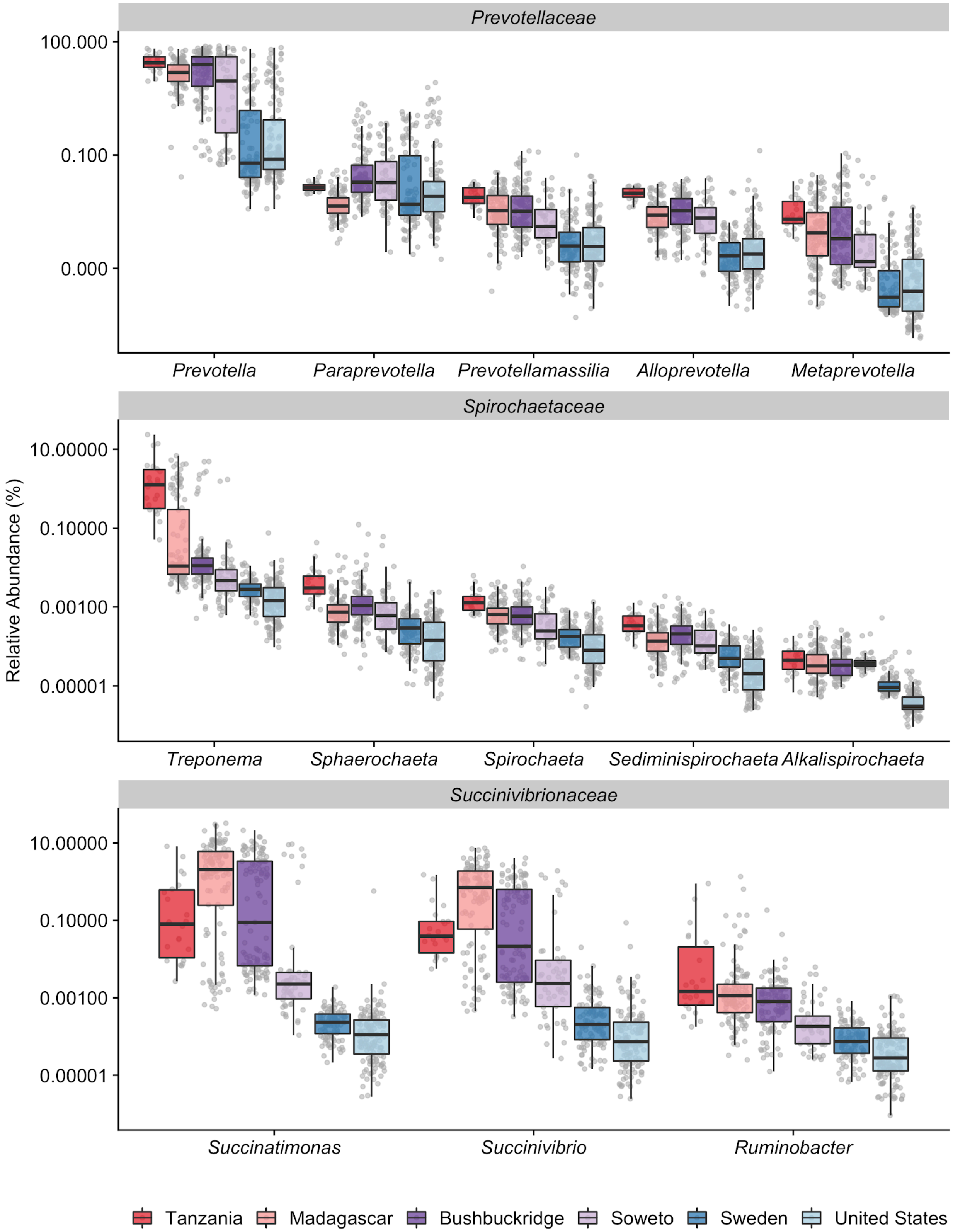

891

892 **Supplementary Figure 8. Relative abundance of VANISH taxa in global cohort**

893 Relative abundance of VANISH genera from the families Prevotellaceae, Spirochaetaceae, and
894 Succinivibrionaceae. A pseudocount of 1 read was added to each sample prior to relative

abundance normalization in order to plot on a log scale. Relative abundance values for most genera trend toward decreasing from nonwestern cohorts to western cohorts.

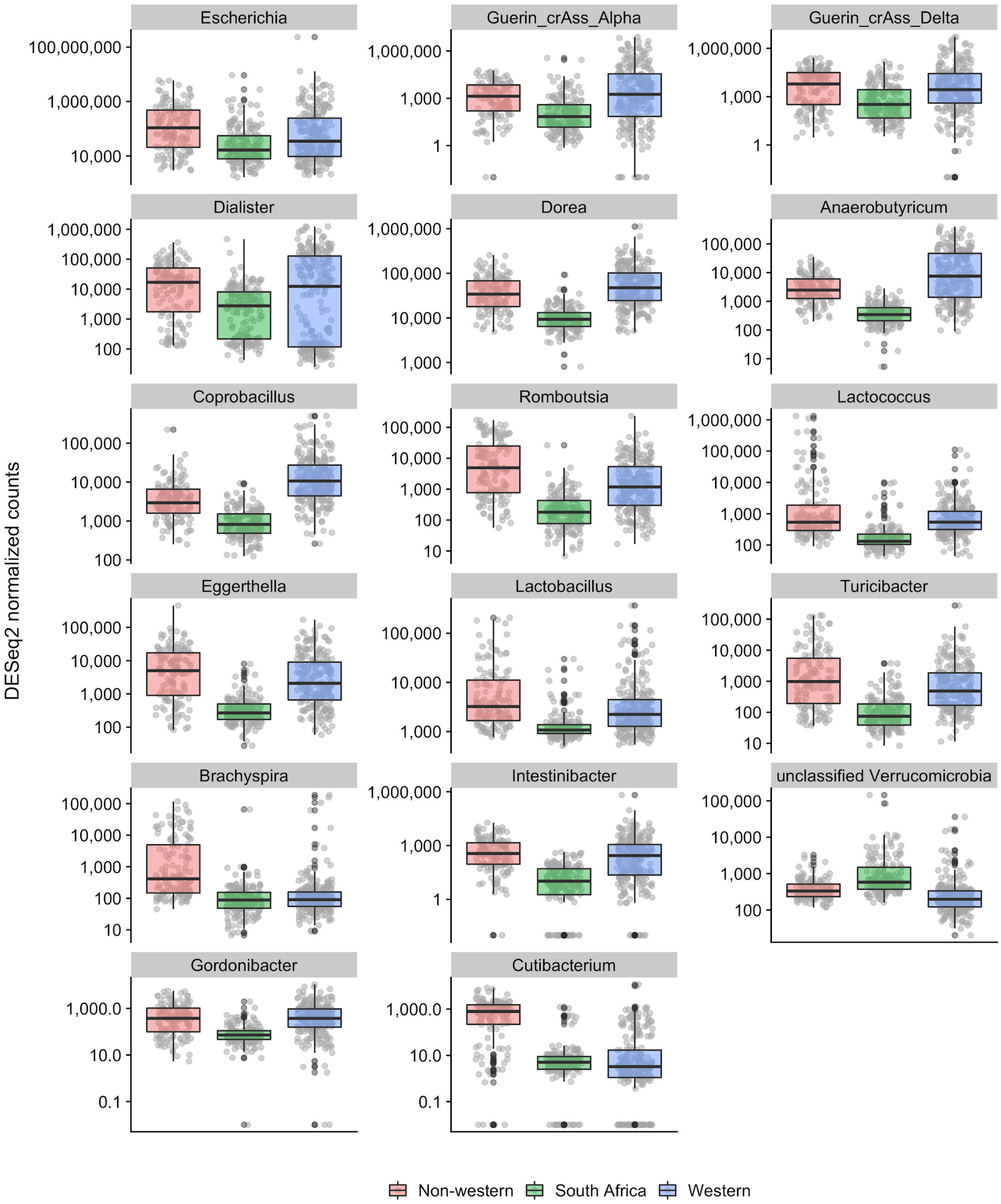

Supplementary Figure 9. Microbial genera which distinguish Bushbuckridge and Soweto

Samples were grouped by geographic region into “western” (USA, Sweden), “nonwestern” (Tanzania, Madagascar) and “South African” (Bushbuckridge, Soweto) and taxa which distinguish the South African group from the western and nonwestern groups were determined separately using DESeq2. Results with the same directionality of log2 fold change with respect to South Africa in both comparisons, with a minimum log2 fold change of 2 in each comparison, are shown. A pseudo-count was added to zero values for plotting.

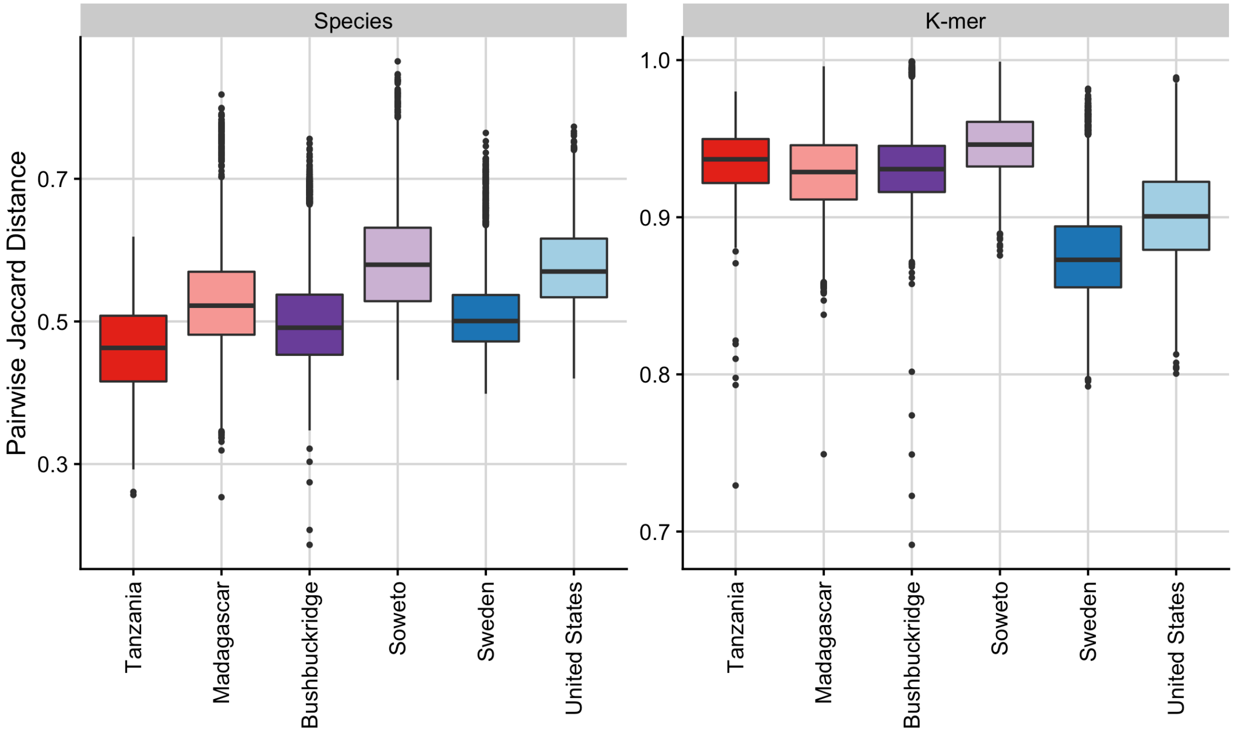

905

906 **Supplementary Figure 10. Cohort-wise beta diversity computed via Jaccard distance**

907 Comparison of pairwise beta diversity within each cohort based on Jaccard distance between

908 species abundance counts and nucleotide *k*-mer sketches. Nonwestern populations have greater

909 beta diversity than western populations considering nucleotide *k*-mer composition.

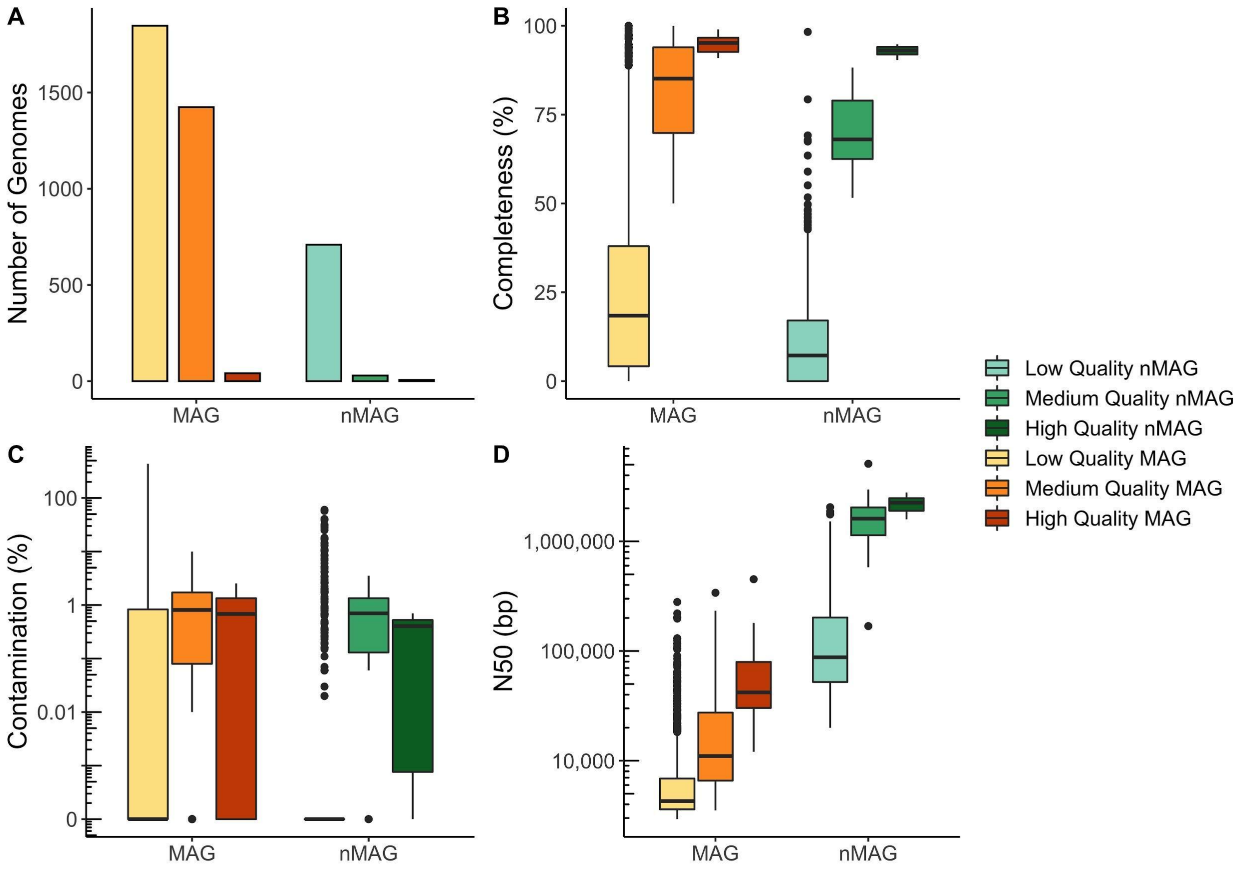

Supplementary Figure 11. Summary statistics for Illumina and nanopore MAGs generated from all samples.

(A) Number of low-, medium-, and high-quality genomes as evaluated with Bowers et al. standards

(B) Distribution of MAG percent completeness as determined by CheckM.

(C) Distribution of MAG percent contamination as determined by CheckM.

(D) Distribution of MAG N50.

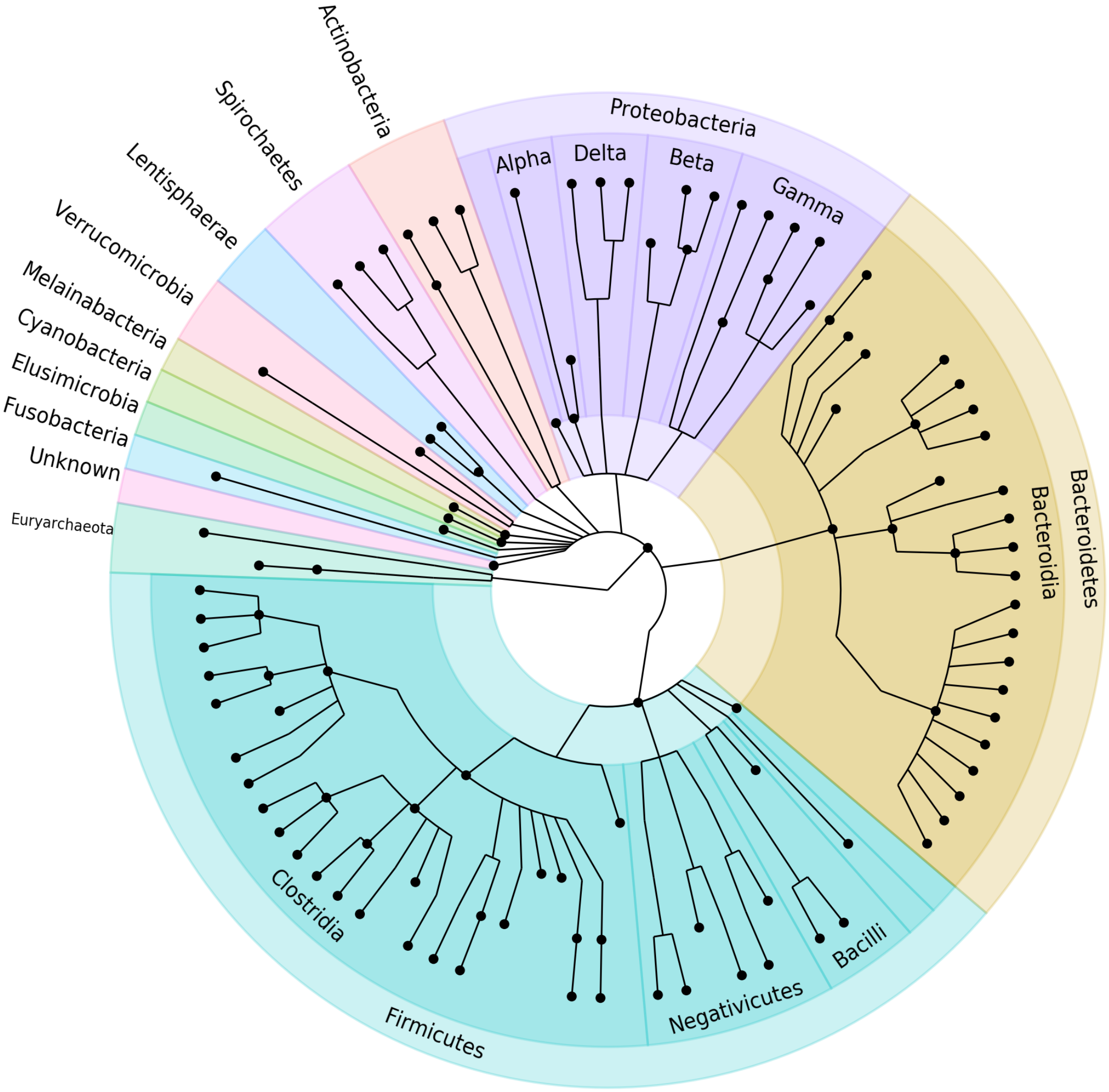

Supplementary Figure 12. Taxonomy of de-replicated Illumina MAGs from all samples

Taxonomic classification of de-replicated medium- and high-quality Illumina MAGs, where black dots indicate a MAG assembled at that level of taxonomic classification. Multiple MAGs at the same classification level are collapsed into single points.

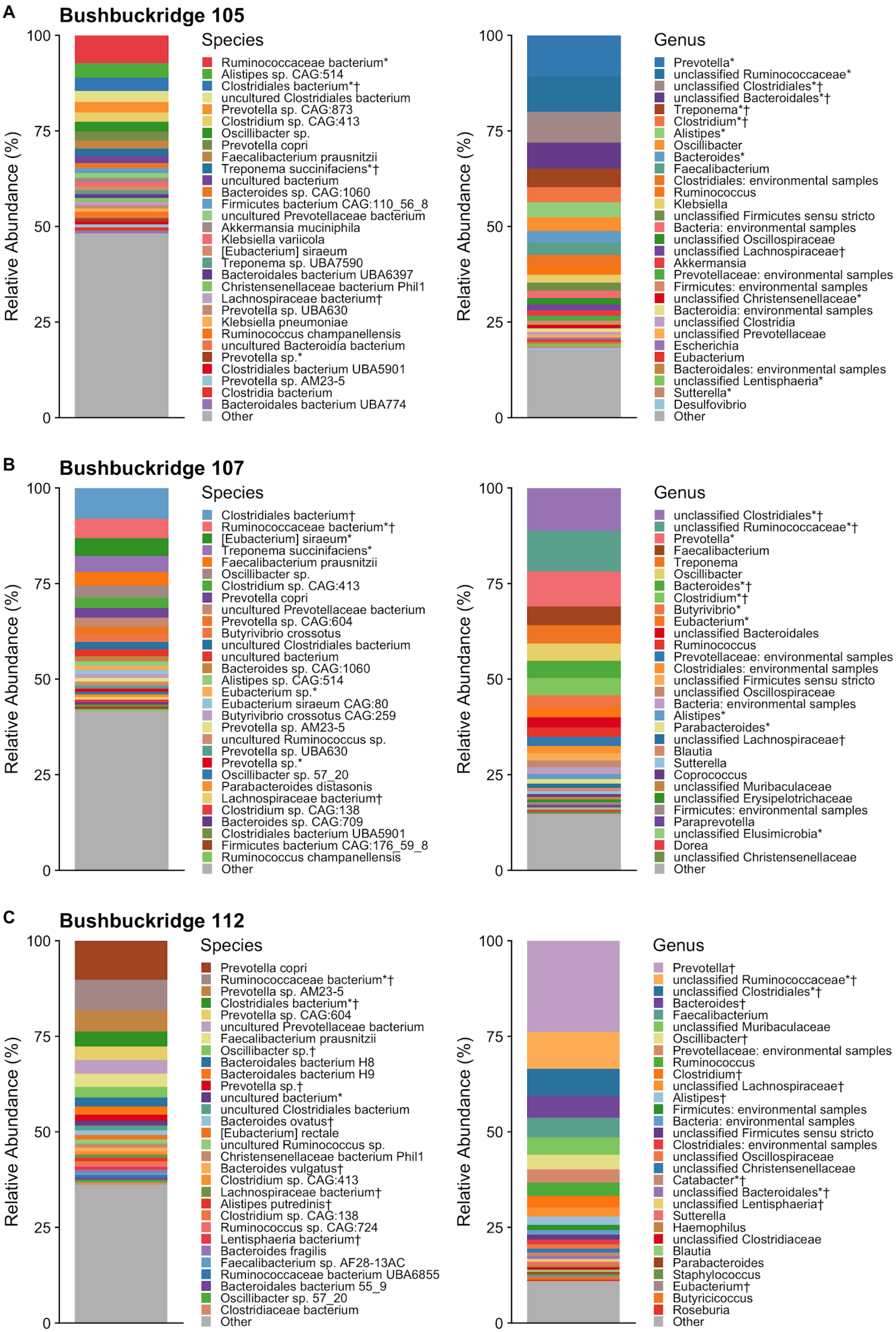
A
Bushbuckridge 105
Relative Abundance (%)
100
75
50
25
0
Species
Ruminococcaceae bacterium*
Alistipes sp. CAG:514
Clostridiales bacterium*†
uncultured Clostridiales bacterium
Prevotella sp. CAG:873
Clostridium sp. CAG:413
Oscillibacter sp.
Prevotella copri
Faecalibacterium prausnitzii
Treponema succinifaciens*†
uncultured bacterium
Bacteroides sp. CAG:1060
Firmicutes bacterium CAG:110_56_8
uncultured Prevotellaceae bacterium
Akkermansia muciniphila
Klebsiella variicola
[Eubacterium] siraeum
Treponema sp. UBA7590
Bacteroidales bacterium UBA6397
Christensenellaceae bacterium Phil1
Lachnospiraceae bacterium†
Prevotella sp. UBA630
Klebsiella pneumoniae
Ruminococcus champanellensis
uncultured Bacteroidia bacterium
Prevotella sp.*
Clostridiales bacterium UBA5901
Prevotella sp. AM23-5
Clostridia bacterium
Bacteroidales bacterium UBA774
Other
Relative Abundance (%)
100
75
50
25
0
Genus
Prevotella*
unclassified Ruminococcaceae*
unclassified Clostridiales*†
unclassified Bacteroidales*†
Treponema*†
Clostridium*†
Alistipes*
Oscillibacter
Bacteroides*
Faecalibacterium
Clostridiales: environmental samples
Ruminococcus
Klebsiella
unclassified Firmicutes sensu stricto
Bacteria: environmental samples
unclassified Oscillospiraceae
unclassified Lachnospiraceae†
Akkermansia
Prevotellaceae: environmental samples
Firmicutes: environmental samples
unclassified Christensenellaceae*
Bacteroidia: environmental samples
unclassified Clostridia
unclassified Prevotellaceae
Escherichia
Eubacterium
Bacteroidales: environmental samples
unclassified Lentisphaeria*
Sutterella*
Desulfovibrio
Other
B
Bushbuckridge 107
Relative Abundance (%)
100
75
50
25
0
Species
Clostridiales bacterium†
Ruminococcaceae bacterium*†
[Eubacterium] siraeum*
Treponema succinifaciens*
Faecalibacterium prausnitzii
Oscillibacter sp.
Clostridium sp. CAG:413
Prevotella copri
uncultured Prevotellaceae bacterium
Prevotella sp. CAG:604
Butyrivibrio crossotus
uncultured Clostridiales bacterium
uncultured bacterium
Bacteroides sp. CAG:1060
Alistipes sp. CAG:514
Eubacterium sp.*
Eubacterium siraeum CAG:80
Butyrivibrio crossotus CAG:259
Prevotella sp. AM23-5
uncultured Ruminococcus sp.
Prevotella sp. UBA630
Prevotella sp.*
Oscillibacter sp. 57_20
Parabacteroides distasonis
Lachnospiraceae bacterium†
Clostridium sp. CAG:138
Bacteroides sp. CAG:709
Clostridiales bacterium UBA5901
Firmicutes bacterium CAG:176_59_8
Ruminococcus champanellensis
Other
Relative Abundance (%)
100
75
50
25
0
Genus
unclassified Clostridiales*†
unclassified Ruminococcaceae*†
Prevotella*
Faecalibacterium
Treponema
Oscillibacter
Bacteroides*†
Clostridium*†
Butyrivibrio*
Eubacterium*
unclassified Bacteroidales
Ruminococcus
Prevotellaceae: environmental samples
Clostridiales: environmental samples
unclassified Firmicutes sensu stricto
unclassified Oscillospiraceae
Bacteria: environmental samples
Alistipes*
Parabacteroides*
unclassified Lachnospiraceae†
Blautia
Sutterella
Coprococcus
unclassified Muribaculaceae
unclassified Erysipelotrichaceae
Firmicutes: environmental samples
Paraprevotella
unclassified Elusimicrobia*
Dorea
unclassified Christensenellaceae
Other
C
Bushbuckridge 112
Relative Abundance (%)
100
75
50
25
0
Species
Prevotella copri
Ruminococcaceae bacterium*†
Prevotella sp. AM23-5
Clostridiales bacterium*†
Prevotella sp. CAG:604
uncultured Prevotellaceae bacterium
Faecalibacterium prausnitzii
Oscillibacter sp.†
Bacteroidales bacterium H8
Bacteroidales bacterium H9
Prevotella sp.†
uncultured bacterium*
uncultured Clostridiales bacterium
Bacteroides ovatus†
[Eubacterium] rectale
uncultured Ruminococcus sp.
Christensenellaceae bacterium Phil1
Bacteroides vulgatus†
Clostridium sp. CAG:413
Lachnospiraceae bacterium†
Alistipes putredinis†
Clostridium sp. CAG:138
Ruminococcus sp. CAG:724
Lentisphaeria bacterium†
Bacteroides fragilis
Faecalibacterium sp. AF28-13AC
Ruminococcaceae bacterium UBA6855
Bacteroidales bacterium 55_9
Oscillibacter sp. 57_20
Clostridiaceae bacterium
Other
Relative Abundance (%)
100
75
50
25
0
Genus
Prevotella†
unclassified Ruminococcaceae*†
unclassified Clostridiales*†
Bacteroides†
Faecalibacterium
unclassified Muribaculaceae
Oscillibacter†
Prevotellaceae: environmental samples
Ruminococcus
Clostridium†
unclassified Lachnospiraceae†
Alistipes†
Firmicutes: environmental samples
Bacteria: environmental samples
unclassified Firmicutes sensu stricto
Clostridiales: environmental samples
unclassified Oscillospiraceae
unclassified Christensenellaceae
Catabacter*†
unclassified Bacteroidales*†
unclassified Lentisphaeria†
Sutterella
Haemophilus
unclassified Clostridiaceae
Blautia
Parabacteroides
Staphylococcus
Eubacterium†
Butyricicoccus
Roseburia
Other

Supplementary Figure 13. Taxonomic composition for samples selected for nanopore sequencing

Short-read sequencing-based taxonomic classifications for the three samples selected for Nanopore sequencing, showing (A) genus-level and (B) species-level classifications. Top thirty taxa by relative abundance shown in each plot. Symbols indicate whether a medium- or high-quality short-read (*) or nanopore MAG (†) was assembled from the corresponding genus or species

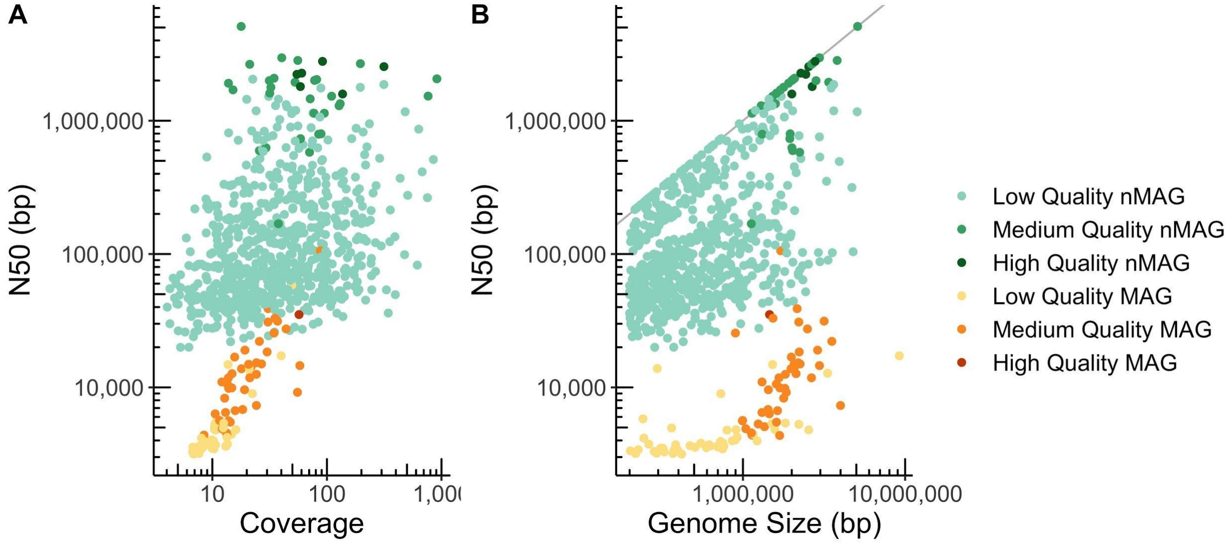

Supplementary Figure 14. Summary statistics of nanopore and short read MAGs generated for three Bushbuckridge samples

(A) MAG short read or long-read coverage versus MAG N50.

(B) MAG total size versus MAG N50. Grey line indicates where genome N50 equals total genome size.

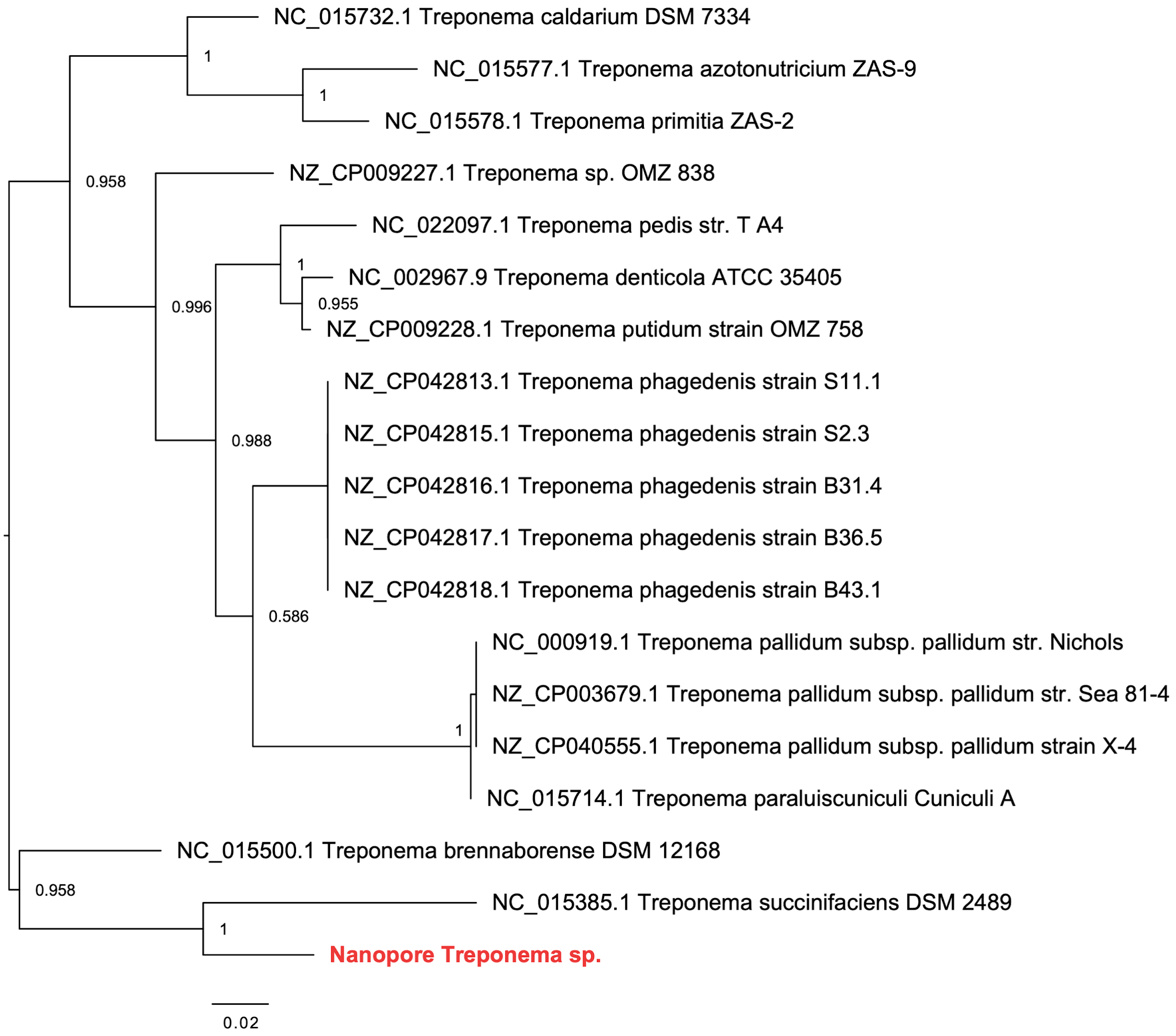
NC_015732.1 Treponema caldarium DSM 7334
NC_015577.1 Treponema azotonutricium ZAS-9
NC_015578.1 Treponema primitia ZAS-2
NZ_CP009227.1 Treponema sp. OMZ 838
NC_022097.1 Treponema pedis str. T A4
NC_002967.9 Treponema denticola ATCC 35405
NZ_CP009228.1 Treponema putidum strain OMZ 758
NZ_CP042813.1 Treponema phagedenis strain S11.1
NZ_CP042815.1 Treponema phagedenis strain S2.3
NZ_CP042816.1 Treponema phagedenis strain B31.4
NZ_CP042817.1 Treponema phagedenis strain B36.5
NZ_CP042818.1 Treponema phagedenis strain B43.1
NC_000919.1 Treponema pallidum subsp. pallidum str. Nichols
NZ_CP003679.1 Treponema pallidum subsp. pallidum str. Sea 81-4
NZ_CP040555.1 Treponema pallidum subsp. pallidum strain X-4
NC_015714.1 Treponema paraluiscuniculi Cuniculi A
NC_015500.1 Treponema brennaborense DSM 12168
NC_015385.1 Treponema succinifaciens DSM 2489
Nanopore Treponema sp.
1
1
0.958
1
0.955
0.996
0.988
0.586
1
0.958
1
0.02

Supplementary Figure 15. Phylogeny of *Treponema* 16S rRNA sequences

Phylogeny of 16S rRNA sequences from species of the genus *Treponema* show that the *Treponema* sp. assembled via Nanopore sequencing is most related to *T. succinifaciens*, but is phylogenetically distinct. The nanopore genome is highlighted in red font. Branch labels indicate Shimodaira-Hasegawa support values for splits.

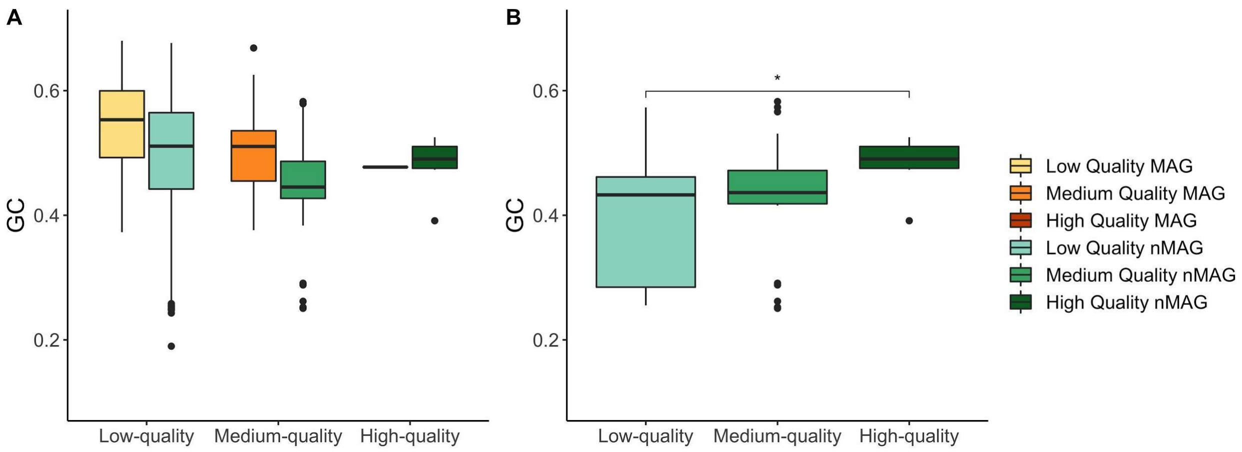

Supplementary Figure 16. GC content of MAGs and nMAGs generated from three Bushbuckridge samples

(A) GC content range of MAGs and nMAGs.

(B) nMAGs with contig N50 values greater than one megabase. GC content of low-quality nMAGs is lower than the GC content of high-quality nMAGs, despite nMAGs of all quality having N50 values of higher than one megabase. * = $p \leq 0.05$, Wilcoxon rank sum test.

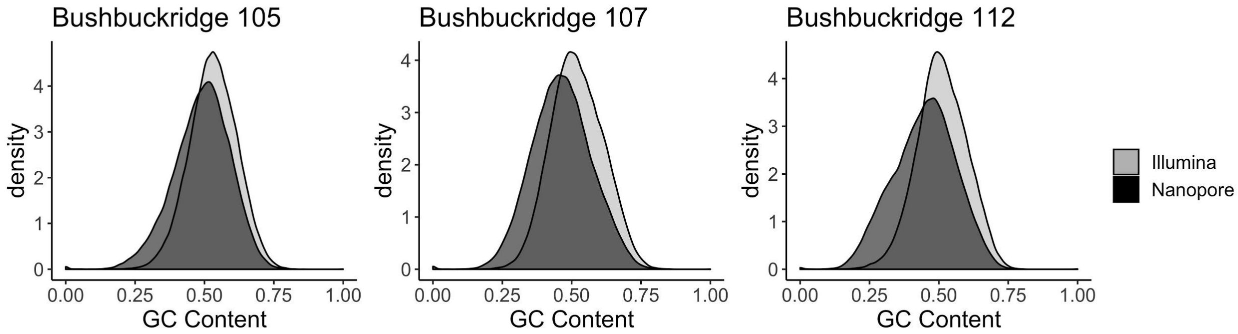

952

953 **Supplementary Figure 17. GC content of nanopore and Illumina sequencing reads**
954 **generated from three Bushbuckridge samples**
955 GC content was calculated for all processed Illumina reads (average length of 126 bp) and for
956 126 bp windows of all nanopore reads. GC content distribution was subsampled to 100,000
957 measurements per method.

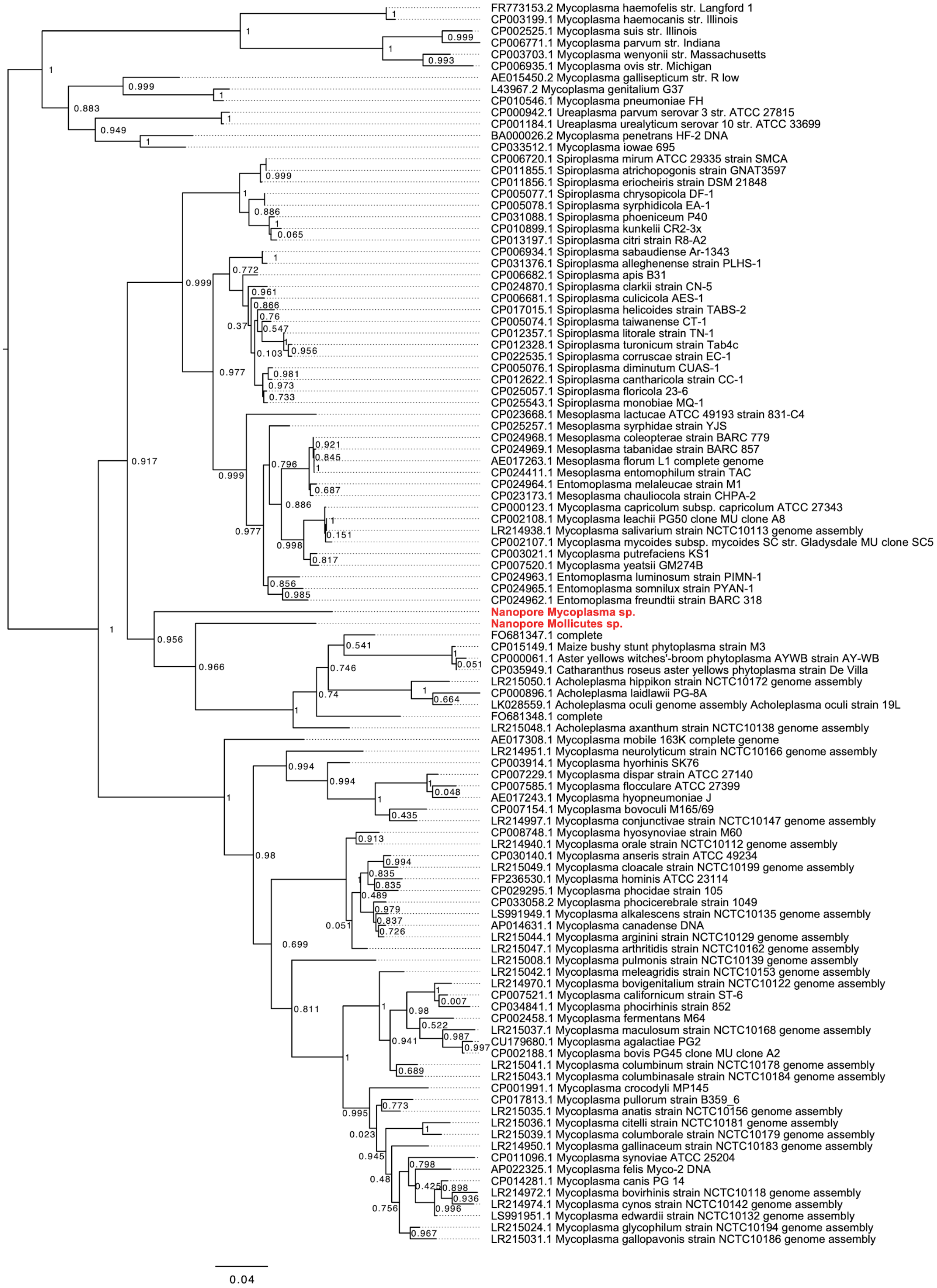
FR773153.2 Mycoplasma haemofelis str. Langford 1
CP003199.1 Mycoplasma haemocanis str. Illinois
CP002525.1 Mycoplasma suis str. Illinois
CP006771.1 Mycoplasma parvum str. Indiana
CP003703.1 Mycoplasma wenyonii str. Massachusetts
CP006935.1 Mycoplasma ovis str. Michigan
AE015450.2 Mycoplasma gallisepticum str. R low
L43967.2 Mycoplasma genitalium G37
CP010546.1 Mycoplasma pneumoniae FH
CP000942.1 Ureaplasma parvum serovar 3 str. ATCC 27815
CP001184.1 Ureaplasma urealyticum serovar 10 str. ATCC 33699
BA000026.2 Mycoplasma penetrans HF-2 DNA
CP033512.1 Mycoplasma iowae 695
CP006720.1 Spiroplasma mirum ATCC 29335 strain SMCA
CP011855.1 Spiroplasma atrichopogonis strain GNAT3597
CP011856.1 Spiroplasma eriocheiris strain DSM 21848
CP005077.1 Spiroplasma chrysopicola DF-1
CP005078.1 Spiroplasma syrphidicola EA-1
CP031088.1 Spiroplasma phoeniceum P40
CP010899.1 Spiroplasma kunkelii CR2-3x
CP013197.1 Spiroplasma citri strain R8-A2
CP006934.1 Spiroplasma sabaudiense Ar-1343
CP031376.1 Spiroplasma alleghenense strain PLHS-1
CP006682.1 Spiroplasma apis B31
CP024870.1 Spiroplasma clarkii strain CN-5
CP006681.1 Spiroplasma culicicola AES-1
CP017015.1 Spiroplasma helicoides strain TABS-2
CP005074.1 Spiroplasma taiwanense CT-1
CP012357.1 Spiroplasma litorale strain TN-1
CP012328.1 Spiroplasma turonicum strain Tab4c
CP022535.1 Spiroplasma corruscae strain EC-1
CP005076.1 Spiroplasma diminutum CUAS-1
CP012622.1 Spiroplasma cantharicola strain CC-1
CP025057.1 Spiroplasma floricola 23-6
CP025543.1 Spiroplasma monobiae MQ-1
CP023668.1 Mesoplasma lactucae ATCC 49193 strain 831-C4
CP025257.1 Mesoplasma syrphidae strain YJS
CP024968.1 Mesoplasma coleopterae strain BARC 779
CP024969.1 Mesoplasma tabanidae strain BARC 857
AE017263.1 Mesoplasma florum L1 complete genome
CP024411.1 Mesoplasma entomophilum strain TAC
CP024964.1 Entomoplasma melaleucae strain M1
CP023173.1 Mesoplasma chauliocola strain CHPA-2
CP000123.1 Mycoplasma capricolum subsp. capricolum ATCC 27343
CP002108.1 Mycoplasma leachii PG50 clone MU clone A8
LR214938.1 Mycoplasma salivarium strain NCTC10113 genome assembly
CP002107.1 Mycoplasma mycoides subsp. mycoides SC str. Gladysdale MU clone SC5
CP003021.1 Mycoplasma putrefaciens KS1
CP007520.1 Mycoplasma yeatsii GM274B
CP024963.1 Entomoplasma luminosum strain PIMN-1
CP024965.1 Entomoplasma somnilux strain PYAN-1
CP024962.1 Entomoplasma freundtii strain BARC 318
Nanopore Mycoplasma sp.
Nanopore Mollicutes sp.
FO681347.1 complete
CP015149.1 Maize bushy stunt phytoplasma strain M3
CP000061.1 Aster yellows witches'-broom phytoplasma AYWB strain AY-WB
CP035949.1 Catharanthus roseus aster yellows phytoplasma strain De Villa
LR215050.1 Acholeplasma hippikon strain NCTC10172 genome assembly
CP000896.1 Acholeplasma laidlawii PG-8A
LK028559.1 Acholeplasma oculi genome assembly Acholeplasma oculi strain 19L
FO681348.1 complete
LR215048.1 Acholeplasma axanthum strain NCTC10138 genome assembly
AE017308.1 Mycoplasma mobile 163K complete genome
LR214951.1 Mycoplasma neurolyticum strain NCTC10166 genome assembly
CP003914.1 Mycoplasma hyorhinis SK76
CP007229.1 Mycoplasma dispar strain ATCC 27140
CP007585.1 Mycoplasma flocculare ATCC 27399
AE017243.1 Mycoplasma hyopneumoniae J
CP007154.1 Mycoplasma bovoculi M165/69
LR214997.1 Mycoplasma conjunctivae strain NCTC10147 genome assembly
CP008748.1 Mycoplasma hyosynoviae strain M60
LR214940.1 Mycoplasma orale strain NCTC10112 genome assembly
CP030140.1 Mycoplasma anseris strain ATCC 49234
LR215049.1 Mycoplasma cloacale strain NCTC10199 genome assembly
FP236530.1 Mycoplasma hominis ATCC 23114
CP029295.1 Mycoplasma phocidae strain 105
CP033058.2 Mycoplasma phocicerebrale strain 1049
LS991949.1 Mycoplasma alkalescens strain NCTC10135 genome assembly
AP014631.1 Mycoplasma canadense DNA
LR215044.1 Mycoplasma arginini strain NCTC10129 genome assembly
LR215047.1 Mycoplasma arthritidis strain NCTC10162 genome assembly
LR215008.1 Mycoplasma pulmonis strain NCTC10139 genome assembly
LR215042.1 Mycoplasma meleagridis strain NCTC10153 genome assembly
LR214970.1 Mycoplasma bovigenitalium strain NCTC10122 genome assembly
CP007521.1 Mycoplasma californicum strain ST-6
CP034841.1 Mycoplasma phocirhinis strain 852
CP002458.1 Mycoplasma fermentans M64
LR215037.1 Mycoplasma maculosum strain NCTC10168 genome assembly
CU179680.1 Mycoplasma agalactiae PG2
CP002188.1 Mycoplasma bovis PG45 clone MU clone A2
LR215041.1 Mycoplasma columbinum strain NCTC10178 genome assembly
LR215043.1 Mycoplasma columbinasale strain NCTC10184 genome assembly
CP001991.1 Mycoplasma crocodyli MP145
CP017813.1 Mycoplasma pullorum strain B359_6
LR215035.1 Mycoplasma anatis strain NCTC10156 genome assembly
LR215036.1 Mycoplasma citelli strain NCTC10181 genome assembly
LR215039.1 Mycoplasma columborale strain NCTC10179 genome assembly
LR214950.1 Mycoplasma gallinaceum strain NCTC10183 genome assembly
CP011096.1 Mycoplasma synoviae ATCC 25204
AP022325.1 Mycoplasma felis Myco-2 DNA
CP014281.1 Mycoplasma canis PG 14
LR214972.1 Mycoplasma bovirhinis strain NCTC10118 genome assembly
LR214974.1 Mycoplasma cynos strain NCTC10142 genome assembly
LS991951.1 Mycoplasma edwardii strain NCTC10132 genome assembly
LR215024.1 Mycoplasma glycophilum strain NCTC10194 genome assembly
LR215031.1 Mycoplasma gallopavonis strain NCTC10186 genome assembly
1
1
0.999
1
0.993
1
0.999
1
0.883
1
0.949
1
0.999
1
0.886
1
0.065
1
0.772
0.999
0.961
0.866
0.76
0.37
0.547
1
0.956
0.103
0.977
0.981
0.973
0.733
0.921
0.845
0.917
0.796
1
0.999
0.687
0.886
1
0.977
0.151
0.998
0.817
0.856
0.985
1
0.956
0.541
1
0.051
0.966
0.746
1
0.74
0.664
1
0.994
0.994
1
0.048
1
1
0.435
0.913
0.98
0.994
0.835
0.835
0.489
0.979
0.837
0.051
0.726
0.699
1
0.007
1
0.811
0.98
0.522
0.987
0.941
0.997
1
0.689
0.773
0.995
1
0.023
0.945
0.798
0.48
0.425
0.898
0.936
0.756
0.996
0.967
0.04

Supplementary Figure 18. Phylogeny of Mollicutes 16S rRNA sequences

Phylogeny of 16S rRNA sequences from species of the class Mollicutes showing the Mollicutes and Mycoplasma genomes assembled via nanopore sequencing. Nanopore genomes are highlighted in red font. Branch labels indicate Shimodaira-Hasegawa support values for splits.

References

Ahlmann-Eltze, C. (2019). ggsignif: Significance Brackets for "ggplot2."

Ajayi, I.O., Adebamowo, C., Adami, H.-O., Dalal, S., Diamond, M.B., Bajunirwe, F., Guwatudde, D., Njelekela, M., Nankya-Mutyoba, J., Chiwanga, F.S., et al. (2016). Urban-rural and geographic differences in overweight and obesity in four sub-Saharan African adult populations: a multi-country cross-sectional study. BMC Public Health *16*, 1126.

Almeida, A., Mitchell, A.L., Boland, M., Forster, S.C., Gloor, G.B., Tarkowska, A., Lawley, T.D., and Finn, R.D. (2019). A new genomic blueprint of the human gut microbiota. Nature *568*, 499–504.

Angelakis, E., Bachar, D., Yasir, M., Musso, D., Djossou, F., Gaborit, B., Brah, S., Diallo, A., Ndombe, G.M., Mediannikov, O., et al. (2019). Treponema species enrich the gut microbiota of traditional rural populations but are absent from urban individuals. New Microbes New Infect *27*, 14–21.

Asnicar, F., Weingart, G., Tickle, T.L., Huttenhower, C., and Segata, N. (2015). Compact graphical representation of phylogenetic data and metadata with GraPhlAn. PeerJ *3*, e1029.

Bäckhed, F., Roswall, J., Peng, Y., Feng, Q., Jia, H., Kovatcheva-Datchary, P., Li, Y., Xia, Y., Xie, H., Zhong, H., et al. (2015). Dynamics and Stabilization of the Human Gut Microbiome during the First Year of Life. Cell Host Microbe *17*, 690–703.

Bishara, A., Moss, E.L., Kolmogorov, M., Parada, A.E., Weng, Z., Sidow, A., Dekas, A.E., Batzoglou, S., and Bhatt, A.S. (2018). High-quality genome sequences of uncultured microbes by assembly of read clouds. Nat. Biotechnol.

Bolourian, A., and Mojtahedi, Z. (2018). Streptomyces, shared microbiome member of soil and gut, as "old friends" against colon cancer. FEMS Microbiology Ecology *94*.

Bowers, R.M., Kyrpides, N.C., Stepanauskas, R., Harmon-Smith, M., Doud, D., Reddy, T.B.K., Schulz, F., Jarett, J., Rivers, A.R., Eloe-Fadrosh, E.A., et al. (2017). Minimum information about a single amplified genome (MISAG) and a metagenome-assembled genome (MIMAG) of bacteria and archaea. Nat. Biotechnol. *35*, 725–731.

Brewster, R., Tamburini, F.B., Asiimwe, E., Oduaran, O., Hazelhurst, S., and Bhatt, A.S. (2019). Surveying Gut Microbiome Research in Africans: Toward Improved Diversity and Representation. Trends Microbiol.

Brito, I.L., Gurry, T., Zhao, S., Huang, K., Young, S.K., Shea, T.P., Naisilisili, W., Jenkins, A.P., Jupiter, S.D., Gevers, D., et al. (2019). Transmission of human-associated microbiota along family and social networks. Nat Microbiol *4*, 964–971.

Brown, C.T., and Irber, L. (2016). sourmash: a library for MinHash sketching of DNA. JOSS *1*, 27.

Campbell, T.P., Sun, X., Patel, V.H., Sanz, C., Morgan, D., and Dantas, G. (2020). The microbiome and resistome of chimpanzees, gorillas, and humans across host lifestyle and geography. ISME J. *14*, 1584–1599.

Ciabattini, A., Olivieri, R., Lazzeri, E., and Medaglini, D. (2019). Role of the Microbiota in the Modulation of Vaccine Immune Responses. Front. Microbiol. *10*, 1305.

Cole, J.R., Wang, Q., Fish, J.A., Chai, B., McGarrell, D.M., Sun, Y., Brown, C.T., Porras-Alfaro, A., Kuske, C.R., and Tiedje, J.M. (2014). Ribosomal Database Project: data and tools for high throughput rRNA analysis. Nucleic Acids Res. *42*, D633–D642.

Collinson, M.A., White, M.J., Bocquier, P., McGarvey, S.T., Afolabi, S.A., Clark, S.J., Kahn, K., and Tollman, S.M. (2014). Migration and the epidemiological transition: insights from the Agincourt sub-district of northeast South Africa. Glob. Health Action *7*, 23514.

Crusoe, M.R., Alameldin, H.F., Awad, S., Boucher, E., Caldwell, A., Cartwright, R., Charbonneau, A., Constantinides, B., Edvenson, G., Fay, S., et al. (2015). The khmer software package: enabling efficient nucleotide sequence analysis. F1000Res. *4*, 900.

de la Cuesta-Zuluaga, J., Corrales-Agudelo, V., Velásquez-Mejía, E.P., Carmona, J.A., Abad, J.M., and Escobar, J.S. (2018). Gut microbiota is associated with obesity and cardiometabolic disease in a population in the midst of Westernization. Sci. Rep. *8*, 11356.

De Filippo, C., Cavalieri, D., Di Paola, M., Ramazzotti, M., Poullet, J.B., Massart, S., Collini, S., Pieraccini, G., and Lionetti, P. (2010). Impact of diet in shaping gut microbiota revealed by a comparative study in children from Europe and rural Africa. Proc. Natl. Acad. Sci. U. S. A. *107*, 14691–14696.

Di Rienzi, S.C., Sharon, I., Wrighton, K.C., Koren, O., Hug, L.A., Thomas, B.C., Goodrich, J.K., Bell, J.T., Spector, T.D., Banfield, J.F., et al. (2013). The human gut and groundwater harbor non-photosynthetic bacteria belonging to a new candidate phylum sibling to Cyanobacteria. Elife *2*, e01102.

Edgar, R.C. (2004). MUSCLE: multiple sequence alignment with high accuracy and high throughput. Nucleic Acids Res. *32*, 1792–1797.

Edwards, R.A., Vega, A.A., Norman, H.M., Ohaeri, M., Levi, K., Dinsdale, E.A., Cinek, O., Aziz, R.K., McNair, K., Barr, J.J., et al. (2019). Global phylogeography and ancient evolution of the widespread human gut virus crAssphage. Nat Microbiol *4*, 1727–1736.

Fragiadakis, G.K., Smits, S.A., Sonnenburg, E.D., Van Treuren, W., Reid, G., Knight, R., Manjurano, A., Changalucha, J., Dominguez-Bello, M.G., Leach, J., et al. (2018). Links between environment, diet, and the hunter-gatherer microbiome. Gut Microbes *10*, 216–227.

Gentleman, R., Carey, V., Huber, W., and Hahne, F. (2019). genefilter: genefilter: methods for filtering genes from high-throughput experiments.

Ginsburg, C., Collinson, M.A., Iturralde, D., van Tonder, L., Gómez-Olivé, F.X., Kahn, K., and Tollman, S. (2016). Migration and Settlement Change in South Africa: Triangulating Census 2011 with Longitudinal Data from the Agincourt Health and Demographic Surveillance System in the Rural North-east. South. Afr. J. Demogr. *17*, 133–198.

Gonçalves da Silva, A. (2017). harrietr: Wrangle Phylogenetic Distance Matrices and Other Utilities.

Gorvitovskaia, A., Holmes, S.P., and Huse, S.M. (2016). Interpreting Prevotella and Bacteroides as biomarkers of diet and lifestyle. Microbiome *4*, 15.

Griffiths, J.A., and Mazmanian, S.K. (2018). Emerging evidence linking the gut microbiome to neurologic disorders. Genome Medicine *10*.

Guerin, E., Shkoporov, A., Stockdale, S.R., Clooney, A.G., Ryan, F.J., Sutton, T.D.S., Draper, L.A., Gonzalez-Tortuero, E., Ross, R.P., and Hill, C. (2018). Biology and Taxonomy of crAss-like Bacteriophages, the Most Abundant Virus in the Human Gut. Cell Host Microbe.

Gupta, V.K., Paul, S., and Dutta, C. (2017). Geography, Ethnicity or Subsistence-Specific Variations in Human Microbiome Composition and Diversity. Front. Microbiol. *8*, 1162.

Gurevich, A., Saveliev, V., Vyahhi, N., and Tesler, G. (2013). QUAST: quality assessment tool for genome assemblies. Bioinformatics *29*, 1072–1075.

Hagan, T., Cortese, M., Rouphael, N., Boudreau, C., Linde, C., Maddur, M.S., Das, J., Wang, H., Guthmiller, J., Zheng, N.-Y., et al. (2019). Antibiotics-Driven Gut Microbiome Perturbation Alters Immunity to Vaccines in Humans. Cell *178*, 1313–1328.e13.

Han, C., Gronow, S., Teshima, H., Lapidus, A., Nolan, M., Lucas, S., Hammon, N., Deshpande, S., Cheng, J.-F., Zeytun, A., et al. (2011). Complete genome sequence of Treponema succinifaciens type strain (6091). Stand. Genomic Sci. *4*, 361–370.

Hansen, M.E.B., Rubel, M.A., Bailey, A.G., Ranciaro, A., Thompson, S.R., Campbell, M.C., Beggs, W., Dave, J.R., Mokone, G.G., Mpoloka, S.W., et al. (2019). Population structure of human gut bacteria in a diverse cohort from rural Tanzania and Botswana. Genome Biol. *20*, 16.

Helmink, B.A., Wadud Khan, M.A., Hermann, A., Gopalakrishnan, V., and Wargo, J.A. (2019). The microbiome, cancer, and cancer therapy. Nature Medicine *25*, 377–388.

Human Microbiome Project Consortium (2012). Structure, function and diversity of the healthy human microbiome. Nature *486*, 207–214.

Hunt, M., Silva, N.D., Otto, T.D., Parkhill, J., Keane, J.A., and Harris, S.R. (2015). Circlator: automated circularization of genome assemblies using long sequencing reads. Genome Biol. *16*, 294.

Jha, A.R., Davenport, E.R., Gautam, Y., Bhandari, D., Tandukar, S., Ng, K.M., Fragiadakis, G.K., Holmes, S., Gautam, G.P., Leach, J., et al. (2018). Gut microbiome transition across a lifestyle gradient in Himalaya. PLoS Biol. *16*, e2005396.

Kabudula, C.W., Houle, B., Collinson, M.A., Kahn, K., Gómez-Olivé, F.X., Clark, S.J., and Tollman, S. (2017a). Progression of the epidemiological transition in a rural South African setting: findings from population surveillance in Agincourt, 1993--2013. BMC Public Health *17*, 424.

Kabudula, C.W., Houle, B., Collinson, M.A., Kahn, K., Gómez-Olivé, F.X., Tollman, S., and Clark, S.J. (2017b). Socioeconomic differences in mortality in the antiretroviral therapy era in Agincourt, rural South Africa, 2001-13: a population surveillance analysis. Lancet Glob Health *5*, e924–e935.

Kang, D.D., Froula, J., Egan, R., and Wang, Z. (2015). MetaBAT, an efficient tool for accurately reconstructing single genomes from complex microbial communities. PeerJ *3*, e1165.

Kassambara, A. (2020). ggpubr: “ggplot2” Based Publication Ready Plots.

Koslicki, D., and Falush, D. (2016). MetaPalette: a -mer Painting Approach for Metagenomic Taxonomic Profiling and Quantification of Novel Strain Variation. mSystems *1*.

Krueger, F. Trim Galore!

Laslett, D., and Canback, B. (2004). ARAGORN, a program to detect tRNA genes and tmRNA genes in nucleotide sequences. Nucleic Acids Res. *32*, 11–16.

Leung, J.M., Graham, A.L., and Knowles, S.C.L. (2018). Parasite-Microbiota Interactions With the Vertebrate Gut: Synthesis Through an Ecological Lens. Front. Microbiol. *9*, 843.

Li, H. (2018). Minimap2: pairwise alignment for nucleotide sequences. Bioinformatics *34*, 3094–3100.

Li, H., and Durbin, R. (2009). Fast and accurate short read alignment with Burrows–Wheeler transform. Bioinformatics.

Li, D., Luo, R., Liu, C.-M., Leung, C.-M., Ting, H.-F., Sadakane, K., Yamashita, H., and Lam, T.-W. (2016). MEGAHIT v1.0: A fast and scalable metagenome assembler driven by advanced methodologies and community practices. Methods *102*, 3–11.

Lim, S.S., Vos, T., Flaxman, A.D., Danaei, G., Shibuya, K., Adair-Rohani, H., Amann, M., Anderson, H.R., Andrews, K.G., Aryee, M., et al. (2012). A comparative risk assessment of burden of disease and injury attributable to 67 risk factors and risk factor clusters in 21 regions, 1990-2010: a systematic analysis for the Global Burden of Disease Study 2010. Lancet *380*, 2224–2260.

Lin, Y., Yuan, J., Kolmogorov, M., Shen, M.W., Chaisson, M., and Pevzner, P.A. (2016). Assembly of long error-prone reads using de Bruijn graphs. Proc. Natl. Acad. Sci. U. S. A. *113*, E8396–E8405.

Lokmer, A., Cian, A., Froment, A., Gantois, N., Viscogliosi, E., Chabé, M., and Ségurel, L. (2019). Use of shotgun metagenomics for the identification of protozoa in the gut microbiota of healthy individuals from worldwide populations with various industrialization levels. PLoS One *14*, e0211139.

Love, M.I., Huber, W., and Anders, S. (2014). Moderated estimation of fold change and dispersion for RNA-seq data with DESeq2. Genome Biol. *15*, 550.

Lu, J., Breitwieser, F.P., Thielen, P., and Salzberg, S.L. (2017). Bracken: estimating species abundance in metagenomics data. PeerJ Comput. Sci. *3*, e104.

Maier, L., and Typas, A. (2017). Systematically investigating the impact of medication on the gut microbiome. Curr. Opin. Microbiol. *39*, 128–135.

Martin, M. (2011). Cutadapt removes adapter sequences from high-throughput sequencing reads. EMBnet.journal *17*, 10–12.

Martínez, I., Stegen, J.C., Maldonado-Gómez, M.X., Eren, A.M., Siba, P.M., Greenhill, A.R., and Walter, J. (2015). The gut microbiota of rural papua new guineans: composition, diversity patterns, and ecological processes. Cell Rep. *11*, 527–538.

Moss, E.L., Maghini, D.G., and Bhatt, A.S. (2020). Complete, closed bacterial genomes from microbiomes using nanopore sequencing. Nat. Biotechnol.

Nayfach, S., Shi, Z.J., Seshadri, R., Pollard, K.S., and Kyrpides, N.C. (2019). New insights from uncultivated genomes of the global human gut microbiome. Nature *568*, 505–510.

NCD Risk Factor Collaboration (NCD-RisC) – Africa Working Group (2017). Trends in obesity and diabetes across Africa from 1980 to 2014: an analysis of pooled population-based studies. Int. J. Epidemiol. *46*, 1421–1432.

Obregon-Tito, A.J., Tito, R.Y., Metcalf, J., Sankaranarayanan, K., Clemente, J.C., Ursell, L.K., Zech Xu, Z., Van Treuren, W., Knight, R., Gaffney, P.M., et al. (2015). Subsistence strategies in traditional societies distinguish gut microbiomes. Nat. Commun. *6*, 6505.

Oduaran, O.H., Tamburini, F.B., Sahibdeen, V., Brewster, R., Gómez-Olivé, F.X., Kahn, K., Norris, S.A., Tollman, S.M., Twine, R., Wade, A.N., et al. (2020). Gut Microbiome Profiling of a Rural and Urban South African Cohort Reveals Biomarkers of a Population in Lifestyle Transition. Biorxiv.

Oksanen, J., Blanchet, F.G., Friendly, M., Kindt, R., Legendre, P., McGlinn, D., Minchin, P.R., O'Hara, R.B., Simpson, G.L., Solymos, P., et al. (2019). vegan: Community Ecology Package.

Olm, M.R., Brown, C.T., Brooks, B., and Banfield, J.F. (2017). dRep: a tool for fast and accurate genomic comparisons that enables improved genome recovery from metagenomes through de-replication. ISME J. *11*, 2864–2868.

Ou, J., Carbonero, F., Zoetendal, E.G., DeLany, J.P., Wang, M., Newton, K., Gaskins, H.R., and O'Keefe, S.J.D. (2013). Diet, microbiota, and microbial metabolites in colon cancer risk in rural Africans and African Americans. Am. J. Clin. Nutr. *98*, 111–120.

Parks, D.H., Imelfort, M., Skennerton, C.T., Hugenholtz, P., and Tyson, G.W. (2015). CheckM: assessing the quality of microbial genomes recovered from isolates, single cells, and metagenomes. Genome Res. *25*, 1043–1055.

Parks, D.H., Rinke, C., Chuvochina, M., Chaumeil, P.-A., Woodcroft, B.J., Evans, P.N., Hugenholtz, P., and Tyson, G.W. (2017). Recovery of nearly 8,000 metagenome-assembled genomes substantially expands the tree of life. Nat Microbiol *2*, 1533–1542.

Parks, D.H., Chuvochina, M., Chaumeil, P.-A., Rinke, C., Mussig, A.J., and Hugenholtz, P. (2020). A complete domain-to-species taxonomy for Bacteria and Archaea. Nat. Biotechnol. *38*, 1079–1086.

Pasolli, E., Asnicar, F., Manara, S., Zolfo, M., Karcher, N., Armanini, F., Beghini, F., Manghi, P., Tett, A., Ghensi, P., et al. (2019). Extensive Unexplored Human Microbiome Diversity Revealed by Over 150,000 Genomes from Metagenomes Spanning Age, Geography, and Lifestyle. Cell *176*, 649–662.e20.

Paulson, J.N., Stine, O.C., Bravo, H.C., and Pop, M. (2013). Differential abundance analysis for microbial marker-gene surveys. Nat. Methods *10*, 1200–1202.

Price, M.N., Dehal, P.S., and Arkin, A.P. (2010). FastTree 2--approximately maximum-likelihood trees for large alignments. PLoS One *5*, e9490.

Qin, J., Li, R., Raes, J., Arumugam, M., Burgdorf, K.S., Manichanh, C., Nielsen, T., Pons, N., Levenez, F., Yamada, T., et al. (2010). A human gut microbial gene catalogue established by metagenomic sequencing. Nature *464*, 59–65.

Rampelli, S., Schnorr, S.L., Consolandi, C., Turroni, S., Severgnini, M., Peano, C., Brigidi, P., Crittenden, A.N., Henry, A.G., and Candela, M. (2015). Metagenome Sequencing of the Hadza Hunter-Gatherer Gut Microbiota. Curr. Biol. *25*, 1682–1693.

Ramsay, M., Crowther, N., Tambo, E., Agongo, G., Baloyi, V., Dikotope, S., Gómez-Olivé, X., Jaff, N., Sorgho, H., Wagner, R., et al. (2016). The AWI-Gen Collaborative Centre: Understanding the interplay between Genomic and Environmental Risk Factors for Cardiometabolic Diseases in sub-Saharan Africa. Global Health, Epidemiology and Genomics.

R Core Team (2019). R: A Language and Environment for Statistical Computing.

Richter, L., Norris, S., Pettifor, J., Yach, D., and Cameron, N. (2007). Cohort Profile: Mandela's children: the 1990 Birth to Twenty study in South Africa. Int. J. Epidemiol. *36*, 504–511.

Rothschild, D., Weissbrod, O., Barkan, E., Kurilshikov, A., Korem, T., Zeevi, D., Costea, P.I., Godneva, A., Kalka, I.N., Bar, N., et al. (2018). Environment dominates over host genetics in shaping human gut microbiota. Nature *555*, 210–215.

Santosa, A., and Byass, P. (2016). Diverse Empirical Evidence on Epidemiological Transition in Low-

and Middle-Income Countries: Population-Based Findings from INDEPTH Network Data. PLoS One *11*, e0155753.

Sato, M.P., Ogura, Y., Nakamura, K., Nishida, R., Gotoh, Y., Hayashi, M., Hisatsune, J., Sugai, M., Takehiko, I., and Hayashi, T. (2019). Comparison of the sequencing bias of currently available library preparation kits for Illumina sequencing of bacterial genomes and metagenomes. DNA Res. *26*, 391–398.

Scher, J.U., Sczesnak, A., Longman, R.S., Segata, N., Ubeda, C., Bielski, C., Rostron, T., Cerundolo, V., Pamer, E.G., Abramson, S.B., et al. (2013). Expansion of intestinal Prevotella copri correlates with enhanced susceptibility to arthritis. Elife *2*, e01202.

Schnorr, S.L., Candela, M., Rampelli, S., Centanni, M., Consolandi, C., Basaglia, G., Turroni, S., Biagi, E., Peano, C., Severgnini, M., et al. (2014). Gut microbiome of the Hadza hunter-gatherers. Nat. Commun. *5*, 3654.

Seemann, T. (2014). Prokka: rapid prokaryotic genome annotation. Bioinformatics *30*, 2068–2069.

Slowikowski, K. (2020). ggrepel: Automatically Position Non-Overlapping Text Labels with “ggplot2.”

Smits, S.A., Leach, J., Sonnenburg, E.D., Gonzalez, C.G., Lichtman, J.S., Reid, G., Knight, R., Manjurano, A., Changalucha, J., Elias, J.E., et al. (2017). Seasonal cycling in the gut microbiome of the Hadza hunter-gatherers of Tanzania. Science *357*, 802–806.

Sonnenburg, E.D., and Sonnenburg, J.L. (2019). The ancestral and industrialized gut microbiota and implications for human health. Nat. Rev. Microbiol. *17*, 383–390.

Sonnenburg, J., and Sonnenburg, E. (2018). A Microbiota Assimilation. Cell Metab. *28*, 675–677.

Soo, R.M., Skennerton, C.T., Sekiguchi, Y., Imelfort, M., Paech, S.J., Dennis, P.G., Steen, J.A., Parks, D.H., Tyson, G.W., and Hugenholtz, P. (2014). An expanded genomic representation of the phylum cyanobacteria. Genome Biol. Evol. *6*, 1031–1045.

Statistics South Africa (2012). Census 2011 Statistical Release.

Stewart, R.D., Auffret, M.D., Warr, A., Walker, A.W., Roehe, R., and Watson, M. (2019). Compendium of 4,941 rumen metagenome-assembled genomes for rumen microbiome biology and enzyme discovery. Nat. Biotechnol. *37*, 953–961.

Tett, A., Huang, K.D., Asnicar, F., Fehlner-Peach, H., Pasolli, E., Karcher, N., Armanini, F., Manghi, P., Bonham, K., Zolfo, M., et al. (2019). The Prevotella copri Complex Comprises Four Distinct Clades Underrepresented in Westernized Populations. Cell Host Microbe *26*, 666–679.e7.

Trönnberg, L., Hawksworth, D., Hansen, A., Archer, C., and Stenström, T.A. (2010). Household-based prevalence of helminths and parasitic protozoa in rural KwaZulu-Natal, South Africa, assessed from faecal vault sampling. Trans. R. Soc. Trop. Med. Hyg. *104*, 646–652.

Turnbaugh, P.J., Hamady, M., Yatsunenko, T., Cantarel, B.L., Duncan, A., Ley, R.E., Sogin, M.L., Jones, W.J., Roe, B.A., Affourtit, J.P., et al. (2009). A core gut microbiome in obese and lean twins. Nature *457*, 480–484.

Tyler, A.D., Mataseje, L., Urfano, C.J., Schmidt, L., Antonation, K.S., Mulvey, M.R., and Corbett, C.R. (2018). Evaluation of Oxford Nanopore’s MinION Sequencing Device for Microbial Whole Genome Sequencing Applications. Sci. Rep. *8*, 10931.

Vangay, P., Johnson, A.J., Ward, T.L., Al-Ghalith, G.A., Shields-Cutler, R.R., Hillmann, B.M., Lucas, S.K., Beura, L.K., Thompson, E.A., Till, L.M., et al. (2018). US Immigration Westernizes the Human Gut Microbiome. Cell *175*, 962–972.e10.

Vaser, R., Sović, I., Nagarajan, N., and Šikić, M. (2017). Fast and accurate de novo genome assembly from long uncorrected reads. Genome Res. *27*, 737–746.

Venables, W.N., and Ripley, B.D. (2002). Modern Applied Statistics with S.

Walker, B.J., Abeel, T., Shea, T., Priest, M., Abouelliel, A., Sakthikumar, S., Cuomo, C.A., Zeng, Q., Wortman, J., Young, S.K., et al. (2014). Pilon: an integrated tool for comprehensive microbial variant detection and genome assembly improvement. PLoS One *9*, e112963.

Warnes, G.R., Bolker, B., and Lumley, T. (2020). gtools: Various R Programming Tools.

Wickham, H. (2007). Reshaping Data with the reshape Package. J. Stat. Softw. *21*, 1–20.

Wickham, H. (2016). ggplot2: Elegant Graphics for Data Analysis.

Wickham, H., François, R., Henry, L., and Müller, K. (2020). dplyr: A Grammar of Data Manipulation.

Wilke, C.O. (2019). cowplot: Streamlined Plot Theme and Plot Annotations for “ggplot2.”

Wood, D.E., and Salzberg, S.L. (2014). Kraken: ultrafast metagenomic sequence classification using exact alignments. Genome Biol. *15*, R46.

Yatsunenko, T., Rey, F.E., Manary, M.J., Trehan, I., Dominguez-Bello, M.G., Contreras, M., Magris, M., Hidalgo, G., Baldassano, R.N., Anokhin, A.P., et al. (2012). Human gut microbiome viewed across age and geography. Nature *486*, 222–227.